

A NUMERICAL SOLUTION METHOD FOR AN INFINITESIMAL ELASTO-PLASTIC COSSERAT MODEL

PATRIZIO NEFF

*Department of Mathematics, Darmstadt University of Technology
Schlossgartenstrasse 7, 64289 Darmstadt, Germany
neff@mathematik.tu-darmstadt.de*

KRZYSZTOF CHELMIŃSKI

*Faculty of Mathematics, Technical University Warsaw, Poland
kchelmin@mini.pw.edu.pl*

WOLFGANG MÜLLER* and CHRISTIAN WIENERS†

*Faculty of Mathematics, Universität Karlsruhe (TH)
Kaiserstr. 12, 76128 Karlsruhe, Germany
*mueller@math.uni-karlsruhe.de
†wieners@math.uni-karlsruhe.de*

Received 9 August 2006
Revised 28 October 2006
Communicated by K.-J. Bathe

We present a finite element implementation of a Cosserat elasto-plastic model and provide a rigorous numerical analysis of the introduced time-incremental algorithm. The model allows the use of standard tools from convex analysis as known from classical Prandtl-Reuss plasticity. We derive the dual stress formulation and prove that for vanishing Cosserat couple modulus $\mu_c \rightarrow 0$ the classical problem is approximated. Our numerical results show the robustness of the approximation. Notably, for positive couple modulus $\mu_c > 0$ there is no need for a safe-load assumption. For small μ_c the response is numerically indistinguishable from the classical response.

Keywords: Plasticity; polar materials; perfect plasticity; convex analysis; dual formulation; finite elements.

AMS Subject Classification: 65N55, 65F10, 74A35

1. Introduction

This paper addresses a finite element implementation and the numerical analysis of *geometrically linear* generalized continua of *Cosserat micropolar* type for elasto-plasticity. General continuum models involving *independent rotations* as additional degrees of freedom have been first introduced by the Cosserat brothers.¹⁴

Their development has been largely forgotten for decades only to be rediscovered in the beginning of the 60s.^{1,21,23,32,33,44,59,66,71–73} At that time theoretical investigations of non-classical continuum theories were the main motivation.⁴⁰ The Cosserat concept has been generalized in various directions, for an overview of these so-called *microcontinuum* theories, see Refs. 9, 20 and 22.

Among the first contributions extending the Cosserat framework to infinitesimal elasto-plasticity we should mention Refs. 65, 43, 7 and more recent infinitesimal elasto-plastic formulations have been investigated in Refs. 16, 18, 36 and 61. These models directly comprise joint elastic and plastic Cosserat effects. Later, the models have been extended to a finite elasto-plastic setting as well^{24,30,31,62–64,68} and references therein. Most of these extensions directly comprise joint elastic and plastic Cosserat effects as well but we pretend that their physical and mathematical significance is at present much more difficult to assess than models where Cosserat effects are restricted to the elastic response of the material²⁴ and references therein. We will investigate a model of the second type which has been introduced in Refs. 51 and 53 in a finite strain framework. A geometrical linearization of this model has been investigated in Refs. 55 and 57 and is shown to be well-posed also in the rate-independent limit for both quasistatic and dynamic processes.

Apart from the theoretical development, the Cosserat type models are today increasingly advocated as a means to regularize the pathological mesh size dependence of localization computations where shear failure mechanisms^{4,5,13,45,47} play a major role, for applications in plasticity see the non-exhaustive list.^{15,16,17,18,36,61} The occurring mathematical difficulties reflect the physical fact that upon localization the validity limit of the classical continuum models is reached. In models without any internal length the deformation should be homogeneous on the scale of a representative volume element of the material.⁴⁶

The incorporation of a length scale, which is natural in a Cosserat theory, has the potential to remove the mesh sensitivity. The presence of the internal length scale causes the localization zones to have finite width. In an engineering context this has been observed many times^{18,36,37} but a rigorous numerical analysis testifying to this observation is missing. Moreover, the actual length scale of a material is difficult to establish experimentally and theoretically⁴¹ and remains basically an open question as is the determination of other additionally appearing material constants in the Cosserat framework. It is also not entirely clear, how the shear band width depends on the characteristic length.

For the well-known mathematical analysis of infinitesimal, linearly elastic Cosserat micropolar models the reader may consult Refs. 19, 35, 26 and 27. Existence results for a geometrically exact elastic Cosserat model are obtained in Ref. 50.

As far as classical rate-independent (perfect) elasto-plasticity is concerned, we remark that global existence for the displacement has been shown only in a very weak, measure-valued sense (provided a safe-load condition is assumed), while the stresses could be shown to remain in $L_2(\Omega, \text{Sym}(3))$.^{3,12,70} If hardening

or viscosity is added, then global classical solution are found already without safe-load assumption.^{2,11,10} A complete theory for the classical rate-independent case remains, however, elusive, see also the remarks in Ref. 12.

While the infinitesimal Cosserat micropolar elasto-plasticity model in its various versions is interesting mathematically in its own right we concentrate in this contribution on the *regularizing properties* for positive Cosserat couple modulus $\mu_c > 0$ of the model presented in Ref. 55. We emphasize that our non-dissipative formulation seems to provide just the necessary amount of regularization missing in classical perfect plasticity. By looking at the Cosserat couple modulus μ_c as a regularizing parameter instead of a material parameter, we avoid the problematic issue of identifying this parameter in a physically reasonable way. Indeed in Ref. 49 and in Refs. 54, 48 and 52 it is argued that this parameter must be set to zero, if treated as a material parameter. This is at variance with practically all the previous literature in this field. It does not, however, mean that the Cosserat model has lost its physical significance; rather it calls for a geometrically exact treatment as, e.g. done in Ref. 58.

Since we investigate the Cosserat model with respect to its regularizing properties, we shall comment shortly on other ways to remove the mesh-sensitivity of the classical Prandtl–Reuss model. It is well known that adding either hardening or viscosity will remove the sensitivity,³⁴ where in both cases, additional parameters have to be prescribed. Both regularizations will already modify the uniaxial response of the material. This is not the case for the Cosserat model. In this sense, the Cosserat model furnishes a weaker regularization than hardening or viscosity and deserves, therefore, our attention.

Our contribution is organized as follows: first, we recall the linearized elasto-plastic Cosserat model introduced in Refs. 53 and 51 and investigated mathematically in Refs. 55 and 57. We then reformulate the setting in the discrete finite element spaces together with a backward Euler discretization of the plastic flow rule in time.

The novelty in this contribution consists in showing that all classical concepts from convex analysis apply to the classical stress part and to prove that the time incremental problem still has variational structure. The time incremental problem is shown to have unique minimizers (in the case where Dirichlet data for both displacements and microrotations are assumed), and we prove finite element convergence for standard finite element approximations. Formulating for the first time, the dual problem in terms of stresses *and* microrotations, we prove that for $\mu_c \rightarrow 0$ classical perfect plasticity is approximated. This convergence result for the dual, time-incremental problem complements a corresponding approximation result for the primal, time-continuous formulation obtained in Ref. 56.

The previous development is complemented by a Newton-type algorithm for the computation of minimizers of the convex primal problem. Since the first variation of the primal functional is Lipschitz continuous, standard semi-smooth Newton methods can be applied, where the generalized derivative is given by the well-known

consistent tangent in classical plasticity. In the last section, numerical experiments confirm our analytical results (even for more general boundary conditions) and show that our Cosserat plasticity model is more regular than Prandtl–Reuss plasticity and convergent to the classical model for $\mu_c \rightarrow 0$ as indeed it should be for a reasonable approximative theory.

2. An Infinitesimal Elasto-Plastic Cosserat Model

In this section we recall the specific infinitesimal elasto-plastic Cosserat model which is analyzed in Ref. 55, and we derive a discrete formulation. This section does not contain new results; it serves for the clear definition of the problem and for the introduction of the notation.

Data

Let $\Omega \subset \mathbb{R}^d$ ($d = 2, 3$) be the reference configuration (an open and connected set in \mathbb{R}^d with piecewise smooth Lipschitz boundary), and let $\Gamma_D \cup \Gamma_N = \partial\Omega$ be a decomposition of the boundary. We fix a time interval $[0, T]$.

The problem depends on the following data: a prescribed displacement vector

$$\mathbf{u}_D : \Gamma_D \times [0, T] \rightarrow \mathbb{R}^d$$

for the essential boundary conditions on Γ_D , and a load functional

$$\ell(t, \mathbf{v}) = \int_{\Omega} \mathbf{b}(t) \cdot \mathbf{v} \, d\mathbf{x} + \int_{\Gamma_N} \mathbf{t}_N(t) \cdot \mathbf{v} \, d\mathbf{a}, \quad t \in [0, T],$$

depending on body force densities and traction force densities

$$\mathbf{b} : \Omega \times [0, T] \rightarrow \mathbb{R}^d, \quad \mathbf{t}_N : \Gamma_N \times [0, T] \rightarrow \mathbb{R}^d.$$

We start with the initial state $\mathbf{u}_D(0) = \mathbf{0}$, $\mathbf{b}(0) = \mathbf{0}$, $\mathbf{t}_N(0) = \mathbf{0}$.

The material is described by a linear elastic response depending on the Lamé constants $\lambda, \mu > 0$. Furthermore, we consider materials which allow for independent infinitesimal microrotations $\bar{A} \in \mathfrak{so}(d)$, where $\mathfrak{so}(d) = \{\boldsymbol{\tau} \in \mathbb{R}^{d,d} : \boldsymbol{\tau}^T = -\boldsymbol{\tau}\}$ is the Lie-algebra of skew-symmetric matrices.

The symmetric matrices are denoted by $\text{Sym}(d) = \{\boldsymbol{\tau} \in \mathbb{R}^{d,d} : \boldsymbol{\tau}^T = \boldsymbol{\tau}\}$. We have the orthogonality relation

$$\bar{A} : \boldsymbol{\tau} = 0, \quad \bar{A} \in \mathfrak{so}(d), \quad \boldsymbol{\tau} \in \text{Sym}(d),$$

with respect to the inner product $A : B = \sum_{i,j=1}^d A_{ij} B_{ij}$ for $A, B \in \mathbb{R}^{d,d}$. Moreover, we use the norm $|B| = \sqrt{B : B}$ and the decomposition $B = \text{sym}(B) + \text{skew}(B)$ with $\text{sym}(B) = \frac{1}{2}(B + B^T)$ and $\text{skew}(B) = \frac{1}{2}(B - B^T)$.

The coupling of the skew-symmetric part of the displacement gradient $D\mathbf{u}$ and the microrotation \bar{A} is determined by a parameter $\mu_c \geq 0$, called the *Cosserat couple modulus*, and the internal length scale of the microrotations is described by

a parameter $L_c > 0$ describing an internal length. On the Dirichlet boundary we prescribe

$$\bar{A}_D: \Gamma_D \times [0, T] \rightarrow \mathfrak{so}(d).$$

For the formulation of consistent boundary conditions we may assume that the prescribed displacement vector \mathbf{u}_D is extended into Ω such that $\bar{A}_D(\mathbf{x}, t) = \text{skew}(D\mathbf{u}_D(\mathbf{x}, t))$ is well-defined.

Finally, inelastic material behavior is modeled by a convex function

$$\phi: \text{Sym}(d) \rightarrow \mathbb{R},$$

determining the convex set $\mathbf{K} = \{\boldsymbol{\tau} \in \text{Sym}(d): \phi(\boldsymbol{\tau}) \leq 0\}$ of admissible (symmetric elastic) stresses. We assume that ϕ is smooth for $\boldsymbol{\tau} \neq \mathbf{0}$, and we assume $\phi(\mathbf{0}) < 0$.

The basic example is the von Mises flow rule $\phi(\boldsymbol{\tau}) = |\text{dev}(\boldsymbol{\tau})| - K_0$ for a given constant $K_0 > 0$. Here, $\text{dev}: \text{Sym}(d) \rightarrow \text{Sym}(d)$ is the projection orthogonal to the isotropic operator $\frac{1}{d}\mathbf{1} \otimes \mathbf{1}: \text{Sym}(d) \rightarrow \text{Sym}(d)$ defined by $(\frac{1}{d}\mathbf{1} \otimes \mathbf{1}): \boldsymbol{\tau} = \frac{1}{d} \text{tr}(\boldsymbol{\tau})\mathbf{1}$, i.e. we have $\text{dev} = \text{Id} - \frac{1}{d}\mathbf{1} \otimes \mathbf{1}$, i.e. $\text{dev } B = B - \frac{1}{d} \text{tr}(B)\mathbf{1}$, where Id denotes the identity map of $\mathbb{R}^{d,d}$ into itself and $\mathbf{1} = \delta_{ij}$ is the identity tensor in $\mathbb{R}^{d,d}$.

The equations of the infinitesimal elasto-plastic Cosserat model

We want to determine displacements

$$\mathbf{u}: \bar{\Omega} \times [0, T] \rightarrow \mathbb{R}^d,$$

in general *non-symmetric* Cauchy-stresses

$$\boldsymbol{\sigma}: \Omega \times [0, T] \rightarrow \mathbb{R}^{d,d},$$

(skew-symmetric infinitesimal) microrotations

$$\bar{A}: \Omega \times [0, T] \rightarrow \mathfrak{so}(d),$$

(symmetric infinitesimal) plastic strains (no plastic spin: $\text{skew}(\boldsymbol{\varepsilon}_p) = 0$)

$$\boldsymbol{\varepsilon}_p: \Omega \times [0, T] \rightarrow \text{Sym}(d),$$

(with initial state $\boldsymbol{\varepsilon}_p(0) = \mathbf{0}$), and a plastic multiplier

$$\Lambda: \Omega \times [0, T] \rightarrow \mathbb{R}$$

satisfying the essential boundary conditions

$$\begin{aligned} \mathbf{u}(\mathbf{x}, t) &= \mathbf{u}_D(\mathbf{x}, t), & (\mathbf{x}, t) \in \Gamma_D \times [0, T], \\ \bar{A}(\mathbf{x}, t) &= \bar{A}_D(\mathbf{x}, t), & (\mathbf{x}, t) \in \Gamma_D \times [0, T], \end{aligned}$$

the constitutive relation

$$\begin{aligned} \boldsymbol{\sigma}(\mathbf{x}, t) &= 2\mu(\text{sym}(D\mathbf{u}(\mathbf{x}, t)) - \boldsymbol{\varepsilon}_p(\mathbf{x}, t)) + \lambda \text{div}(\mathbf{u})(\mathbf{x}, t)\mathbf{1} \\ &\quad + 2\mu_c(\text{skew}(D\mathbf{u}(\mathbf{x}, t)) - \bar{A}(\mathbf{x}, t)), & (\mathbf{x}, t) \in \Omega \times [0, T], \end{aligned}$$

the equilibrium equations

$$\begin{aligned} -\operatorname{div} \boldsymbol{\sigma}(\mathbf{x}, t) &= \mathbf{b}(\mathbf{x}, t), & (\mathbf{x}, t) \in \Omega \times [0, T], \\ \boldsymbol{\sigma}(\mathbf{x}, t) \mathbf{n}(\mathbf{x}) &= \mathbf{t}_N(\mathbf{x}, t), & (\mathbf{x}, t) \in \Gamma_N \times [0, T], \\ -\mu L_c^2 \Delta \bar{A}(\mathbf{x}, t) &= \mu_c (\operatorname{skew}(D\mathbf{u}(\mathbf{x}, t)) - \bar{A}(\mathbf{x}, t)), & (\mathbf{x}, t) \in \Omega \times [0, T], \\ D\bar{A}(\mathbf{x}, t) \cdot \mathbf{n}(\mathbf{x}) &= \mathbf{0}, & (\mathbf{x}, t) \in \Gamma_N \times [0, T] \end{aligned}$$

(where $\mathbf{n}(\mathbf{x})$ denotes the outer unit normal vector), the flow rule

$$\frac{d}{dt} \boldsymbol{\varepsilon}_p(\mathbf{x}, t) = \Lambda(\mathbf{x}, t) D\phi(T_E(\mathbf{x}, t)), \quad (\mathbf{x}, t) \in \Omega \times [0, T], \tag{2.1}$$

depending (only) on (the symmetric elastic Eshelby stress tensor T_E)

$$T_E(\mathbf{x}, t) = 2\mu (\operatorname{sym}(D\mathbf{u}(\mathbf{x}, t)) - \boldsymbol{\varepsilon}_p(\mathbf{x}, t)), \quad (\mathbf{x}, t) \in \Omega \times [0, T],$$

and the complementary conditions (Karush–Kuhn–Tucker)

$$\begin{aligned} \Lambda(\mathbf{x}, t) \phi(T_E(\mathbf{x}, t)) &= 0, & \Lambda(\mathbf{x}, t) \geq 0, \\ \phi(T_E(\mathbf{x}, t)) &\leq 0, & (\mathbf{x}, t) \in \Omega \times [0, T]. \end{aligned} \tag{2.2}$$

Here and in the following, for $\boldsymbol{\tau} \in \operatorname{Sym}(d)$ the derivative $D\phi(\boldsymbol{\tau}) \in \operatorname{Sym}(d)$ is represented in $\operatorname{Sym}(d)$ such that for the Gâteaux derivative $D\phi(\boldsymbol{\tau})[\boldsymbol{\eta}]$ it holds

$$D\phi(\boldsymbol{\tau}) : \boldsymbol{\eta} = D\phi(\boldsymbol{\tau})[\boldsymbol{\eta}] = \lim_{h \rightarrow 0} \frac{1}{h} (\phi(\boldsymbol{\tau} + h\boldsymbol{\eta}) - \phi(\boldsymbol{\tau})), \quad \boldsymbol{\eta} \in \operatorname{Sym}(d).$$

Remark 2.1. For a given material history $\boldsymbol{\varepsilon}_p(t)$ at fixed time t , the displacement and the microrotation are determined by minimizing the total energy

$$I(\mathbf{u}, \bar{A}, \boldsymbol{\varepsilon}_p) = \mathcal{E}(D\mathbf{u}, \bar{A}, \boldsymbol{\varepsilon}_p) - \ell(t, \mathbf{u}),$$

where the corresponding elastic free energy is given by

$$\begin{aligned} \mathcal{E}(D\mathbf{u}, \bar{A}, \boldsymbol{\varepsilon}_p) &= \mu \int_{\Omega} |\operatorname{sym}(D\mathbf{u}) - \boldsymbol{\varepsilon}_p|^2 d\mathbf{x} + \frac{\lambda}{2} \int_{\Omega} \operatorname{tr}(D\mathbf{u})^2 d\mathbf{x} \\ &\quad + \mu_c \int_{\Omega} |\operatorname{skew}(D\mathbf{u}) - \bar{A}|^2 d\mathbf{x} + \mu L_c^2 \int_{\Omega} |D\bar{A}|^2 d\mathbf{x}. \end{aligned} \tag{2.3}$$

Remark 2.2. Equivalently, the flow rule (2.1) and the complementary condition (2.2) can be formulated using the subdifferential calculus²:

$$\frac{d}{dt} \boldsymbol{\varepsilon}_p(\mathbf{x}, t) \in \partial\chi_{\mathbf{K}}(T_E(\mathbf{x}, t)), \quad (\mathbf{x}, t) \in \Omega \times [0, T],$$

where $\chi_{\mathbf{K}}$ denotes the indicator function of the convex set \mathbf{K} and $\partial\chi_{\mathbf{K}}$ is the multi-valued derivative. For the case $\phi(\boldsymbol{\tau}) = |\boldsymbol{\tau}| - K_0$ we have

$$\partial\chi_{\mathbf{K}}(\boldsymbol{\tau}) = \partial\hat{\chi}_{\mathbf{K}}(|\boldsymbol{\tau}|) \frac{\boldsymbol{\tau}}{|\boldsymbol{\tau}|}, \quad \partial\hat{\chi}_{\mathbf{K}}(|\boldsymbol{\tau}|) = \begin{cases} 0 & |\boldsymbol{\tau}| < K_0, \\ [0, \infty) & |\boldsymbol{\tau}| = K_0, \\ \emptyset & |\boldsymbol{\tau}| > K_0. \end{cases}$$

3. The Discrete Elasto-Plastic Cosserat Model

Discretization in space

Let h be a mesh size parameter, let $\mathbf{V}_h \subset C^{0,1}(\Omega, \mathbb{R}^d)$ be a finite element space, and set

$$\mathbf{V}_h(\mathbf{u}_D) = \{\mathbf{v} \in \mathbf{V}_h : \mathbf{v}(\mathbf{x}) = \mathbf{u}_D(\mathbf{x}) \text{ for } \mathbf{x} \in D_h\},$$

where $D_h \subset \Gamma_D$ is the set of all nodal points on Γ_D .

Analogously, let $W_h \subset C^{0,1}(\Omega, \mathfrak{so}(d))$ be another finite element space, and let

$$W_h(A_D) = \{B \in W_h : B(\mathbf{x}) = A_D(\mathbf{x}) \text{ for } \mathbf{x} \in D'_h\},$$

where $D'_h \subset \Gamma_D$ is the set of all nodal points on Γ_D of W_h .

Let $\Xi_h \subset \Omega$ be quadrature points and let ω_ξ be the corresponding quadrature weights such that

$$\int_{\Omega} \mathbf{v} \cdot \mathbf{w} \, dx = \sum_{\xi \in \Xi_h} \omega_\xi \mathbf{v}(\xi) \cdot \mathbf{w}(\xi), \quad \mathbf{v}, \mathbf{w} \in \mathbf{V}_h.$$

We set $\Lambda = \{\Lambda : \Xi_h \rightarrow \mathbb{R}\}$, $\Sigma_h = \{\boldsymbol{\tau} : \Xi_h \rightarrow \mathbb{R}^{d,d}\}$ and $\mathbf{E}_h^p = \{\boldsymbol{\tau} : \Xi_h \rightarrow \mathfrak{sl}(d) \cap \text{Sym}(d)\}$, where $\mathfrak{sl}(d) = \{\boldsymbol{\tau} \in \mathbb{R}^{d,d} : \text{tr}(\boldsymbol{\tau}) = 0\}$ is the Lie algebra of trace-free matrices.

In our notation the integral is also used for the finite sums

$$\int_{\Omega} \boldsymbol{\sigma} : \boldsymbol{\varepsilon} \, dx := \sum_{\xi \in \Xi_h} \omega_\xi \boldsymbol{\sigma}(\xi) : \boldsymbol{\varepsilon}(\xi), \quad \boldsymbol{\sigma}, \boldsymbol{\varepsilon} \in \Sigma_h.$$

The semi-discrete equations of the elasto-plastic Cosserat model

Determine

- displacements $\mathbf{u} : [0, T] \rightarrow \mathbf{V}_h$ with $\mathbf{u}(t) \in \mathbf{V}_h(\mathbf{u}_D(t))$ for $t \in [0, T]$,
- microrotations $\bar{A} : [0, T] \rightarrow W_h$ with $\bar{A}(t) \in W_h(\bar{A}_D(t))$ for $t \in [0, T]$,
- stresses $\boldsymbol{\sigma} : [0, T] \rightarrow \Sigma_h$,
- plastic strains $\boldsymbol{\varepsilon}_p : [0, T] \rightarrow \mathbf{E}_h^p$,
- plastic multiplier $\Lambda : [0, T] \rightarrow \Lambda$,

satisfying the constitutive relation

$$\begin{aligned} \boldsymbol{\sigma}(\xi, t) &= 2\mu(\text{sym}(D\mathbf{u}(\xi, t)) - \boldsymbol{\varepsilon}_p(\xi, t)) + \lambda \text{div}(\mathbf{u})(\xi, t)\mathbf{1} \\ &\quad + 2\mu_c(\text{skew}(D\mathbf{u})(\xi, t) - \bar{A}(\xi, t)) \end{aligned}$$

for $(\xi, t) \in \Xi_h \times [0, T]$ (using $\boldsymbol{\sigma}(\xi, t) := \boldsymbol{\sigma}(t)(\xi)$ for $\boldsymbol{\sigma}(t) \in \Sigma_h$), the equilibrium equations

$$\int_{\Omega} \boldsymbol{\sigma}(t) : D\mathbf{v} \, dx = \ell(t, \mathbf{v}), \quad t \in [0, T], \quad \mathbf{v} \in \mathbf{V}_h(\mathbf{0}),$$

$$\begin{aligned} & \mu L_c^2 \int_{\Omega} D\bar{A}(t) \cdot D\bar{B} \, d\mathbf{x} \\ & = \mu_c \int_{\Omega} (\text{skew}(D\mathbf{u}(t)) - \bar{A}(t)) : \bar{B} \, d\mathbf{x}, \quad t \in [0, T], \quad \bar{B} \in W_h(\mathbf{0}) \end{aligned}$$

(where $D\bar{A} \cdot D\bar{B} = \sum_{ijk} \partial_i A_{jk} \partial_i B_{jk}$), the flow rule

$$\frac{d}{dt} \varepsilon_p(\boldsymbol{\xi}, t) = \Lambda(\boldsymbol{\xi}, t) D\phi(T_E(\boldsymbol{\xi}, t)), \quad (\boldsymbol{\xi}, t) \in \Xi_h \times [0, T],$$

depending on

$$T_E(\boldsymbol{\xi}, t) = 2\mu(\text{sym}(D\mathbf{u}(\boldsymbol{\xi}, t)) - \varepsilon_p(\boldsymbol{\xi}, t)), \quad (\boldsymbol{\xi}, t) \in \Xi_h \times [0, T],$$

and the complementary conditions (Karush–Kuhn–Tucker)

$$\Lambda(\boldsymbol{\xi}, t) \phi(T_E(\boldsymbol{\xi}, t)) = 0, \quad \Lambda(\boldsymbol{\xi}, t) \geq 0, \quad \phi(T_E(\boldsymbol{\xi}, t)) \leq 0, \quad (\boldsymbol{\xi}, t) \in \Omega \times [0, T].$$

Discretization in time

The model of incremental infinitesimal Cosserat plasticity is obtained by a decomposition

$$0 = t_0 < t_1 < \dots < t_N = T$$

of the time interval and the backward Euler scheme: for $n = 1, 2, 3, \dots$, the next increment depends on the material history described by ε_p^{n-1} (where $\varepsilon_p^0 = \mathbf{0}$ at $t_0 = 0$ is given), the new load $\ell^n[\mathbf{v}] = \ell(t_n, \mathbf{v})$ and the new Dirichlet boundary values $\mathbf{u}_D^n = \mathbf{u}_D(t_n)$ and $\bar{A}_D^n = \bar{A}_D(t_n)$. We compute the displacement $\mathbf{u}^n \in \mathbf{V}_h(\mathbf{u}_D^n)$ satisfying the essential boundary conditions, the stress $\boldsymbol{\sigma}^n \in \boldsymbol{\Sigma}_h$, the microrotation $\bar{A}^n \in W_h(\bar{A}_D^n)$, the plastic strain $\varepsilon_p^n \in \mathbf{E}_h^p$, and the plastic multiplier $\Lambda^n \in \Lambda$ satisfying the constitutive relation

$$\begin{aligned} \boldsymbol{\sigma}^n(\boldsymbol{\xi}) &= 2\mu(\text{sym}(D\mathbf{u}^n(\boldsymbol{\xi})) - \varepsilon_p^n(\boldsymbol{\xi})) + \lambda \text{div}(\mathbf{u}^n)(\boldsymbol{\xi}) \mathbb{1} \\ &+ 2\mu_c(\text{skew}(D\mathbf{u}^n(\boldsymbol{\xi})) - \bar{A}^n(\boldsymbol{\xi})), \quad \boldsymbol{\xi} \in \Xi_h, \end{aligned} \tag{3.1}$$

the equilibrium equations

$$\int_{\Omega} \boldsymbol{\sigma}^n : D\mathbf{v} \, d\mathbf{x} = \ell^n[\mathbf{v}], \quad \mathbf{v} \in \mathbf{V}_h(\mathbf{0}) \tag{3.2a}$$

$$\mu L_c^2 \int_{\Omega} D\bar{A}^n \cdot D\bar{B} \, d\mathbf{x} = \mu_c \int_{\Omega} (\text{skew}(D\mathbf{u}^n) - \bar{A}^n) : \bar{B} \, d\mathbf{x}, \quad \bar{B} \in W_h(\mathbf{0}), \tag{3.2b}$$

the flow rule

$$\frac{1}{t_n - t_{n-1}} (\varepsilon_p^n(\boldsymbol{\xi}) - \varepsilon_p^{n-1}(\boldsymbol{\xi})) = \Lambda^n(\boldsymbol{\xi}) D\phi(T_E^n(\boldsymbol{\xi})), \quad \boldsymbol{\xi} \in \Xi_h,$$

depending on

$$T_E^n(\boldsymbol{\xi}) = 2\mu(\text{sym}(D\mathbf{u}^n(\boldsymbol{\xi})) - \varepsilon_p^n(\boldsymbol{\xi})), \quad \boldsymbol{\xi} \in \Xi_h, \tag{3.3}$$

and the complementary conditions (Karush–Kuhn–Tucker)

$$\Lambda^n(\boldsymbol{\xi}) \phi(T_E^n(\boldsymbol{\xi})) = 0, \quad \Lambda^n(\boldsymbol{\xi}) \geq 0, \quad \phi(T_E^n(\boldsymbol{\xi})) \leq 0, \quad \boldsymbol{\xi} \in \Xi_h.$$

Since the problem is rate-independent, rescaling of the time parameter does not affect the model. Thus, we define $\gamma^n = 2\mu(t_n - t_{n-1})\Lambda^n \in \mathbf{\Lambda}$, i.e. the flow rule has the form

$$\epsilon_p^n(\boldsymbol{\xi}) = \epsilon_p^{n-1}(\boldsymbol{\xi}) + \frac{\gamma^n(\boldsymbol{\xi})}{2\mu} D\phi(T_E^n(\boldsymbol{\xi})), \quad \boldsymbol{\xi} \in \Xi_h. \tag{3.4}$$

Together with (3.1), (3.2) and (3.3), we can state the fully discrete elasto-plastic Cosserat problem: for given $\epsilon_p^{n-1} \in \mathbf{E}_h^p$ find $\boldsymbol{\sigma}^n, T_E^n \in \Sigma_h, \mathbf{u}^n \in \mathbf{V}_h(\mathbf{u}_D^n), \bar{A}^n \in W_h(\bar{A}_D^n)$, and $\gamma^n \in \mathbf{\Lambda}$ such that

$$T_E^n(\boldsymbol{\xi}) = 2\mu(\text{sym}(D\mathbf{u}^n(\boldsymbol{\xi})) - \epsilon_p^{n-1}(\boldsymbol{\xi})) - \gamma^n(\boldsymbol{\xi})D\phi(T_E^n(\boldsymbol{\xi})) \quad \boldsymbol{\xi} \in \Xi_h, \tag{3.5a}$$

$$\phi(T_E^n(\boldsymbol{\xi})) \leq 0, \quad \gamma^n(\boldsymbol{\xi})\phi(T_E^n(\boldsymbol{\xi})) = 0, \quad \gamma^n(\boldsymbol{\xi}) \geq 0, \quad \boldsymbol{\xi} \in \Xi_h, \tag{3.5b}$$

$$\begin{aligned} \boldsymbol{\sigma}^n(\boldsymbol{\xi}) &= T_E^n(\boldsymbol{\xi}) + \lambda \text{div}(\mathbf{u}^n)(\boldsymbol{\xi})\mathbf{1} \\ &\quad + 2\mu_c(\text{skew}(D\mathbf{u}^n(\boldsymbol{\xi})) - \bar{A}^n(\boldsymbol{\xi})), \quad \boldsymbol{\xi} \in \Xi_h, \end{aligned} \tag{3.5c}$$

$$\int_{\Omega} \boldsymbol{\sigma}^n : D\mathbf{v} \, d\mathbf{x} = \ell^n[\mathbf{v}], \quad \mathbf{v} \in \mathbf{V}_h(\mathbf{0}) \tag{3.5d}$$

$$\mu L_c^2 \int_{\Omega} D\bar{A}^n \cdot D\bar{B} \, d\mathbf{x} = \mu_c \int_{\Omega} (\text{skew}(D\mathbf{u}^n) - \bar{A}^n) : \bar{B} \, d\mathbf{x}, \quad \bar{B} \in W_h(\mathbf{0}). \tag{3.5e}$$

Then, for the next time step ϵ_p^n is determined by the discrete flow rule (3.4).

4. The Closest Point Projection

The algorithmic treatment of the incremental plasticity problem relies on equivalent characterizations obtained by the closest point projection of arbitrary stresses to the admissible stresses. Since the set of admissible stresses is convex, the computation of the projection onto this set is a standard problem in convex optimization.

Projection onto the set of admissible stresses

Let $P_{\mathbf{K}} : \text{Sym}(d) \rightarrow \mathbf{K}$ be the orthogonal projection onto the convex set of admissible stresses $\mathbf{K} = \{\boldsymbol{\tau} \in \text{Sym}(d) : \phi(\boldsymbol{\tau}) \leq 0\}$ with respect to the norm $|\boldsymbol{\tau}| = \sqrt{\boldsymbol{\tau} : \boldsymbol{\tau}}$. Note that $\mathbf{0} \in \mathbf{K}$ (since $\phi(\mathbf{0}) < 0$). We assume that ϕ is smooth for $\boldsymbol{\tau} \neq \mathbf{0}$.

Lemma 4.1. *For given $\boldsymbol{\theta} \in \text{Sym}(d)$ the projection $T = P_{\mathbf{K}}(\boldsymbol{\theta}) \in \mathbf{K}$ is uniquely determined by the solution $(T, \gamma) \in \text{Sym}(d) \times \mathbb{R}$ of the KKT-system*

$$0 = T - \boldsymbol{\theta} + \gamma D\phi(T), \tag{4.1a}$$

$$0 \geq \phi(T), \quad \gamma\phi(T) = 0, \quad \gamma \geq 0. \tag{4.1b}$$

Proof. The constraint minimization problem

$$T \in \text{Sym}(d) : \quad \frac{1}{2}|T - \boldsymbol{\theta}|^2 = \min. \quad \text{subject to } \phi(T) \leq 0$$

satisfies the Slater condition (since $\phi(\mathbf{0}) < 0$). Thus, the minimizer is characterized

by a saddle point $(T, \gamma) \in \text{Sym}(d) \times \mathbb{R}$ of the Lagrange functional

$$L(T, \gamma) = \frac{1}{2}|T - \boldsymbol{\theta}|^2 + \gamma \phi(T),$$

and the corresponding KKT-system (4.1). □

The convex potential

The corresponding convex potentials are denoted by

$$\varphi_{\mathbf{K}}(\boldsymbol{\theta}) = \frac{1}{2}|\boldsymbol{\theta} - P_{\mathbf{K}}(\boldsymbol{\theta})|^2, \quad \psi_{\mathbf{K}}(\boldsymbol{\theta}) = \frac{1}{2}|\boldsymbol{\theta}|^2 - \frac{1}{2}|\boldsymbol{\theta} - P_{\mathbf{K}}(\boldsymbol{\theta})|^2,$$

for $\boldsymbol{\theta} \in \text{Sym}(d)$. Note that we have

$$D\varphi_{\mathbf{K}}(\boldsymbol{\theta})[\boldsymbol{\eta}] = (\boldsymbol{\theta} - P_{\mathbf{K}}(\boldsymbol{\theta})) : \boldsymbol{\eta}, \quad \boldsymbol{\theta}, \boldsymbol{\eta} \in \text{Sym}(d). \tag{4.2}$$

Lemma 4.2. *The functional $\psi_{\mathbf{K}}(\cdot)$ is convex, non-negative, and we have*

$$D\psi_{\mathbf{K}}(\boldsymbol{\theta})[\boldsymbol{\eta}] = P_{\mathbf{K}}(\boldsymbol{\theta}) : \boldsymbol{\eta}, \quad \boldsymbol{\theta}, \boldsymbol{\eta} \in \text{Sym}(d). \tag{4.3}$$

Proof. The orthogonal projection $P_{\mathbf{K}}$ is uniquely characterized by

$$(\boldsymbol{\theta} - P_{\mathbf{K}}(\boldsymbol{\theta})) : (\boldsymbol{\eta} - P_{\mathbf{K}}(\boldsymbol{\theta})) \leq 0, \quad \boldsymbol{\theta} \in \text{Sym}(d), \quad \boldsymbol{\eta} \in \mathbf{K}. \tag{4.4}$$

Inserting (4.2) gives $D\psi_{\mathbf{K}}(\boldsymbol{\theta})[\boldsymbol{\eta}] = \boldsymbol{\theta} : \boldsymbol{\eta} - D\varphi_{\mathbf{K}}(\boldsymbol{\theta})[\boldsymbol{\eta}] = P_{\mathbf{K}}(\boldsymbol{\theta}) : \boldsymbol{\eta}$, and we obtain from (4.4) for $\boldsymbol{\theta}, \boldsymbol{\eta} \in \text{Sym}(d)$

$$\begin{aligned} \psi_{\mathbf{K}}(\boldsymbol{\theta}) - \psi_{\mathbf{K}}(\boldsymbol{\eta}) - D\psi_{\mathbf{K}}(\boldsymbol{\eta})[\boldsymbol{\theta} - \boldsymbol{\eta}] &= P_{\mathbf{K}}(\boldsymbol{\theta}) : \boldsymbol{\theta} - \frac{1}{2}P_{\mathbf{K}}(\boldsymbol{\theta}) : P_{\mathbf{K}}(\boldsymbol{\theta}) - P_{\mathbf{K}}(\boldsymbol{\eta}) : \boldsymbol{\eta} \\ &\quad + \frac{1}{2}P_{\mathbf{K}}(\boldsymbol{\eta}) : P_{\mathbf{K}}(\boldsymbol{\eta}) - P_{\mathbf{K}}(\boldsymbol{\eta}) : (\boldsymbol{\theta} - \boldsymbol{\eta}) \\ &= (P_{\mathbf{K}}(\boldsymbol{\theta}) - P_{\mathbf{K}}(\boldsymbol{\eta})) : (\boldsymbol{\theta} - P_{\mathbf{K}}(\boldsymbol{\theta})) \\ &\quad + \frac{1}{2}|P_{\mathbf{K}}(\boldsymbol{\theta}) - P_{\mathbf{K}}(\boldsymbol{\eta})|^2 \\ &\geq \frac{1}{2}|P_{\mathbf{K}}(\boldsymbol{\theta}) - P_{\mathbf{K}}(\boldsymbol{\eta})|^2. \end{aligned}$$

Thus, $D\psi_{\mathbf{K}}(\boldsymbol{\eta})[\boldsymbol{\theta} - \boldsymbol{\eta}] \leq \psi_{\mathbf{K}}(\boldsymbol{\theta}) - \psi_{\mathbf{K}}(\boldsymbol{\eta})$, i.e. $D\psi_{\mathbf{K}}$ is monotone and therefore $\psi_{\mathbf{K}}$ is convex. Finally, since $\mathbf{0} \in \mathbf{K}$ we have

$$\psi_{\mathbf{K}}(\boldsymbol{\theta}) = \frac{1}{2}|\boldsymbol{\theta}|^2 - \frac{1}{2}|\boldsymbol{\theta} - P_{\mathbf{K}}(\boldsymbol{\theta})|^2 \geq \frac{1}{2}|\boldsymbol{\theta}|^2 - \frac{1}{2}|\boldsymbol{\theta} - \mathbf{0}|^2 = 0. \tag{4.5} \quad \square$$

Example

We consider the evaluation of the projection for the classical von Mises flow rule $\phi(T) = |\text{dev}(T)| - K_0$ for given (yield stress) $K_0 > 0$. For $\boldsymbol{\theta} \in \mathbf{K}$ we have $T = \boldsymbol{\theta}$

and $\gamma = 0$. Otherwise, the KKT-system

$$\begin{aligned} 0 &= T - \boldsymbol{\theta} + \gamma \frac{\text{dev}(T)}{|\text{dev}(T)|}, \\ 0 &= |\text{dev}(T)| - K_0 \end{aligned}$$

has a unique solution, and using $\text{dev}(\boldsymbol{\theta}) = \left(1 + \frac{\gamma}{|\text{dev}(T)|}\right) \text{dev}(T)$ we obtain^{25,60}

$$\begin{aligned} P_{\mathbf{K}}(\boldsymbol{\theta}) &= \boldsymbol{\theta} - \max\{0, |\text{dev}(\boldsymbol{\theta})| - K_0\} \frac{\text{dev}(\boldsymbol{\theta})}{|\text{dev}(\boldsymbol{\theta})|}, \\ \gamma &= \max\{0, |\text{dev}(\boldsymbol{\theta})| - K_0\}, \\ \psi_{\mathbf{K}}(\boldsymbol{\theta}) &= \begin{cases} \frac{1}{2} |\boldsymbol{\theta}|^2 & |\text{dev}(\boldsymbol{\theta})| \leq K_0, \\ \frac{1}{2} \left(\frac{1}{d} \text{tr}(\boldsymbol{\theta})^2 + 2K_0 |\text{dev}(\boldsymbol{\theta})| - K_0^2\right) & |\text{dev}(\boldsymbol{\theta})| > K_0. \end{cases} \end{aligned}$$

Defining $m(s) = \max\{0, s\}$ and using

$$\partial m(s) = \begin{cases} 1 & s > 0, \\ [0, 1] & s = 0, \\ 0 & s < 0, \end{cases}$$

we obtain for the multi-valued derivative of the projection

$$\begin{aligned} \partial P_{\mathbf{K}}(\boldsymbol{\theta})[\boldsymbol{\tau}] &= \boldsymbol{\tau} - \partial m(|\text{dev}(\boldsymbol{\theta})| - K_0) \frac{\text{dev}(\boldsymbol{\theta}) : \text{dev}(\boldsymbol{\tau})}{|\text{dev}(\boldsymbol{\theta})|} \frac{\text{dev}(\boldsymbol{\theta})}{|\text{dev}(\boldsymbol{\theta})|} \\ &\quad - m(|\text{dev}(\boldsymbol{\theta})| - K_0) \left(\frac{\text{dev}(\boldsymbol{\tau})}{|\text{dev}(\boldsymbol{\theta})|} - \frac{\text{dev}(\boldsymbol{\theta}) : \text{dev}(\boldsymbol{\tau})}{|\text{dev}(\boldsymbol{\theta})|} \frac{\text{dev}(\boldsymbol{\theta})}{|\text{dev}(\boldsymbol{\theta})|^2} \right), \end{aligned}$$

i.e.

$$\begin{aligned} \partial P_{\mathbf{K}}(\boldsymbol{\theta}) &= \text{Id} - \partial m(|\text{dev}(\boldsymbol{\theta})| - K_0) \frac{\text{dev}(\boldsymbol{\theta})}{|\text{dev}(\boldsymbol{\theta})|} \otimes \frac{\text{dev}(\boldsymbol{\theta})}{|\text{dev}(\boldsymbol{\theta})|} \\ &\quad - \frac{m(|\text{dev}(\boldsymbol{\theta})| - K_0)}{|\text{dev}(\boldsymbol{\theta})|} \left(\left(\text{Id} - \frac{1}{d} \mathbf{1} \otimes \mathbf{1} \right) - \frac{\text{dev}(\boldsymbol{\theta})}{|\text{dev}(\boldsymbol{\theta})|} \otimes \frac{\text{dev}(\boldsymbol{\theta})}{|\text{dev}(\boldsymbol{\theta})|} \right). \end{aligned} \tag{4.5}$$

For the special choice $m'(s) \in \partial m(s)$ defined by

$$m'(s) = \begin{cases} 1 & s > 0, \\ 0 & s \leq 0, \end{cases}$$

we obtain the following realization $\mathbb{C}(\boldsymbol{\theta}) \in \partial P_{\mathbf{K}}(\boldsymbol{\theta})$ for the consistent tangent defined by

$$\mathbb{C}(\boldsymbol{\theta}) = \begin{cases} \text{Id} & |\text{dev}(\boldsymbol{\theta})| \leq K_0, \\ \frac{1}{d} \mathbf{1} \otimes \mathbf{1} + \frac{K_0}{|\text{dev}(\boldsymbol{\theta})|} \left(\left(\text{Id} - \frac{1}{d} \mathbf{1} \otimes \mathbf{1} \right) - \frac{\text{dev}(\boldsymbol{\theta})}{|\text{dev}(\boldsymbol{\theta})|} \otimes \frac{\text{dev}(\boldsymbol{\theta})}{|\text{dev}(\boldsymbol{\theta})|} \right) & |\text{dev}(\boldsymbol{\theta})| > K_0. \end{cases}$$

Note that this coincides with the classical consistent linearization as is defined, e.g. in Refs. 67 and 39.

Since $\mathbb{C}(\boldsymbol{\theta}) \in \partial^2 \psi_{\mathbf{K}}(\boldsymbol{\theta})$ is the second variation of the convex $\psi_{\mathbf{K}}(\cdot)$, the consistent tangent $\mathbb{C}(\boldsymbol{\theta})$ is positive semi-definite. Moreover, we have $\mathbb{C}(\boldsymbol{\theta}) :$

$\text{dev}(\boldsymbol{\theta}) = \mathbf{0}$, i.e. $\mathbb{C}(\boldsymbol{\theta})$ is not positive definite. Furthermore, $\psi_{\mathbf{K}}(\cdot)$ is not strictly convex and it is of asymptotic linear growth.⁶⁰

Note that $m(\cdot)$ and therefore $P_{\mathbf{K}}$ is semi-smooth satisfying

$$\sup_{A \in \partial P_{\mathbf{K}}(\boldsymbol{\theta} + \delta\boldsymbol{\tau})} |P_{\mathbf{K}}(\boldsymbol{\theta} + \delta\boldsymbol{\tau}) - P_{\mathbf{K}}(\boldsymbol{\theta}) - \delta A[\boldsymbol{\tau}]| = o(\delta).$$

As a consequence, the nonlinear problem which will be studied in the next section is semi-smooth as well. Thus, the convergence analysis for generalized Newton methods³⁸ can be applied.

5. Variational Formulation of the Discrete Elasto-Plastic Cosserat Model

Depending on \mathbf{u}^n and $\boldsymbol{\varepsilon}_p^{n-1}$ we define the trial stress

$$\boldsymbol{\theta}^n(\boldsymbol{\xi}) = 2\mu(\text{sym}(D\mathbf{u}^n(\boldsymbol{\xi})) - \boldsymbol{\varepsilon}_p^{n-1}(\boldsymbol{\xi})), \quad \boldsymbol{\xi} \in \Xi_h, \tag{5.1}$$

i.e.

$$T_E^n(\boldsymbol{\xi}) = \boldsymbol{\theta}^n(\boldsymbol{\xi}) - \gamma^n(\boldsymbol{\xi})D\phi(T_E^n(\boldsymbol{\xi})), \quad \boldsymbol{\xi} \in \Xi_h.$$

Lemma 5.1. *The system (3.5) for the discrete elasto-plastic Cosserat model is equivalent to the following nonlinear variational problem:*

for given $\boldsymbol{\varepsilon}_p^{n-1}$ find $(\mathbf{u}^n, \bar{A}^n) \in \mathbf{V}_h(\mathbf{u}_D^n) \times W_h(\bar{A}_D^n)$ such that

$$\int_{\Omega} P_{\mathbf{K}}(2\mu(\text{sym}(D\mathbf{u}^n) - \boldsymbol{\varepsilon}_p^{n-1})) : D\mathbf{v} \, d\mathbf{x} + \lambda \int_{\Omega} \text{div}(\mathbf{u}^n) \text{div}(\mathbf{v}) \, d\mathbf{x} + 2\mu_c \int_{\Omega} (\text{skew}(D\mathbf{u}^n) - \bar{A}^n) : D\mathbf{v} \, d\mathbf{x} = \ell^n[\mathbf{v}], \quad \mathbf{v} \in \mathbf{V}_h(\mathbf{0}), \tag{5.2a}$$

$$\mu L_c^2 \int_{\Omega} D\bar{A}^n \cdot D\bar{B} \, d\mathbf{x} = \mu_c \int_{\Omega} (\text{skew}(D\mathbf{u}^n) - \bar{A}^n) : \bar{B} \, d\mathbf{x}, \quad \bar{B} \in W_h(\mathbf{0}). \tag{5.2b}$$

Proof. Inserting Lemma 4.1 we obtain directly that (3.5a), (3.5b) is equivalent to

$$T_E^n(\boldsymbol{\xi}) = P_{\mathbf{K}}(\boldsymbol{\theta}^n(\boldsymbol{\xi})), \quad \boldsymbol{\xi} \in \Xi_h.$$

Then, (3.5c) gives

$$\boldsymbol{\sigma}^n(\boldsymbol{\xi}) = P_{\mathbf{K}}(\boldsymbol{\theta}^n(\boldsymbol{\xi})) + \lambda \text{div}(\mathbf{u}^n)(\boldsymbol{\xi})\mathbf{1} + 2\mu_c(\text{skew}(D\mathbf{u}^n(\boldsymbol{\xi})) - \bar{A}^n(\boldsymbol{\xi}))$$

for $\boldsymbol{\xi} \in \Xi_h$, and (5.2) follows from (3.5d) and (3.5e). □

It is important to observe that the weak form of the incremental Cosserat problem still has a variational structure in the following sense.

Lemma 5.2. Any minimizer $(\mathbf{u}^n, \bar{A}^n) \in \mathbf{V}_h(\mathbf{u}_D^n) \times W_h(\bar{A}_D^n)$ of the functional

$$I_{\text{incr}}^n(\mathbf{u}, \bar{A}) = \mathcal{E}_{\text{incr}}(D\mathbf{u}, \bar{A}, \boldsymbol{\varepsilon}_p^{n-1}) - \ell^n[\mathbf{u}] \tag{5.3}$$

solves the nonlinear variational problem (5.2). Here $\mathcal{E}_{\text{incr}}$ denotes the free energy of the incremental problem defined by

$$\begin{aligned} \mathcal{E}_{\text{incr}}(D\mathbf{u}, \bar{A}, \boldsymbol{\varepsilon}_p) &= \frac{1}{2\mu} \int_{\Omega} \psi_{\mathbf{K}}(2\mu(\text{sym}(D\mathbf{u}) - \boldsymbol{\varepsilon}_p)) \, d\mathbf{x} + \frac{\lambda}{2} \int_{\Omega} \text{tr}(D\mathbf{u})^2 \, d\mathbf{x} \\ &+ \mu_c \int_{\Omega} |\text{skew}(D\mathbf{u}) - \bar{A}|^2 \, d\mathbf{x} + \mu L_c^2 \int_{\Omega} |D\bar{A}|^2 \, d\mathbf{x}. \end{aligned} \tag{5.4}$$

Note that for the first time step $n = 1$ and $\boldsymbol{\varepsilon}_p^0 = \mathbf{0}$, $\mu_c = 0$, $L_c = 0$ the functional $I_{\text{incr}}^1(\mathbf{u}, \bar{0})$ reduces to the primal plastic functional of static perfect plasticity (Hencky plasticity).^{25,60,69}

Proof. Any minimizer is a critical point, i.e. $DI_{\text{incr}}^n(\mathbf{u}, \bar{A}) = 0$. From (4.3) we obtain for the first variation of I_{incr}^n with respect to \mathbf{u}

$$\begin{aligned} D_1 I_{\text{incr}}^n(\mathbf{u}, \bar{A})[\mathbf{v}] &= \frac{1}{2\mu} \int_{\Omega} P_{\mathbf{K}}(2\mu(\text{sym}(D\mathbf{u}) - \boldsymbol{\varepsilon}_p^{n-1})) : (2\mu \text{sym}(D\mathbf{v})) \, d\mathbf{x} \\ &+ \lambda \int_{\Omega} \text{div}(\mathbf{u}) \text{div}(\mathbf{v}) \, d\mathbf{x} + 2\mu_c \int_{\Omega} (\text{skew}(D\mathbf{u}) - \bar{A}) : \text{skew}(D\mathbf{v}) \, d\mathbf{x} - \ell^n[\mathbf{v}] \end{aligned}$$

which proves (5.2a); analogously $D_2 I_{\text{incr}}^n(\mathbf{u}^n, \bar{A}^n)[\bar{B}] = 0$ gives (5.2b). □

6. Analysis of the Discrete Elasto-Plastic Cosserat Model

For the analysis of the model we restrict ourselves to the pure Dirichlet problem with homogeneous boundary conditions $\mathbf{u}_D \equiv \mathbf{0}$ and $\bar{A}_D \equiv \mathbf{0}$ on $\Gamma_D = \partial\Omega$, to linear finite elements \mathbf{V}_h, W_h , and to mid-point quadrature on the triangles or tetrahedra. Thus, we can identify the discrete stress space $\boldsymbol{\Sigma}_h$ with elementwise constant functions in $L_2(\Omega, \mathbb{R}^{d,d})$. By abuse of notation we set $\mathbf{V}_h := \mathbf{V}_h(\mathbf{0})$ and $W_h := W_h(\mathbf{0})$, so that we have $\mathbf{V}_h \subset \mathbf{V}$ and $W_h \subset W$, where $\mathbf{V} = H_0^1(\Omega, \mathbb{R}^d)$ and $W = H_0^1(\Omega, \mathfrak{so}(d))$. The norm in $L_2(\Omega)$ is denoted by $\|\cdot\|$.

Due to the boundary conditions, Poincaré constants C_0, C_1 exist such that

$$\begin{aligned} \|\mathbf{v}\| &\leq C_0 \|D\mathbf{v}\|, \quad \mathbf{v} \in \mathbf{V}, \\ \|\bar{B}\| &\leq C_1 \|D\bar{B}\|, \quad \bar{B} \in W, \end{aligned} \tag{6.1}$$

and, a constant $C_3 > 0$ exists such that²⁸

$$\|D\mathbf{v}\|^2 \leq C_3 (\|\text{div } \mathbf{v}\|^2 + \|\text{curl } \mathbf{v}\|^2), \quad \mathbf{v} \in \mathbf{V}. \tag{6.2}$$

Note that we have

$$\|\text{div}(\mathbf{v})\|^2 + \|\text{curl}(\mathbf{v})\|^2 = \|\text{tr}(D\mathbf{v})\|^2 + \|\text{skew}(D\mathbf{v})\|^2. \tag{6.3}$$

Finally, we define $\|\ell^n\|_{\mathbf{V}'} = \sup_{\|D\mathbf{v}\|=1} |\ell^n[\mathbf{v}]|$.

Theorem 6.1. *The functional $I_{\text{incr}}^n : \mathbf{V} \times W \rightarrow \mathbb{R}$ in (5.3) is uniformly convex and bounded from below satisfying*

$$I_{\text{incr}}^n(\mathbf{u}, \bar{A}) \geq \mu_c c_4 \left(\|D\mathbf{u}\|^2 + \|D\bar{A}\|^2 \right) - \frac{1}{4\mu_c c_4} \|\ell^n\|_{\mathbf{V}'}^2. \tag{6.4}$$

Moreover, for $\mu_c \in (0, \mu]$ the constant c_4 is independent of μ_c .

Proof. In the first step, we show that the symmetric bilinear form

$$\begin{aligned} b[(\mathbf{u}, \bar{A}), (\mathbf{v}, \bar{B})] &= \lambda \int_{\Omega} \operatorname{div}(\mathbf{u}) \operatorname{div}(\mathbf{v}) \, dx + 2\mu L_c^2 \int_{\Omega} D\bar{A} \cdot D\bar{B} \, dx \\ &\quad + 2\mu_c \int_{\Omega} (\operatorname{skew}(D\mathbf{u}) - \bar{A}) : (\operatorname{skew}(D\mathbf{v}) - \bar{B}) \, dx \end{aligned}$$

induces a coercive quadratic form. Inserting

$$\|\operatorname{skew}(D\mathbf{u}) - \bar{A}\|^2 \geq (1 - \alpha) \|\operatorname{skew}(D\mathbf{u})\|^2 + \left(1 - \frac{1}{\alpha}\right) \|\bar{A}\|^2,$$

with $\alpha \in (0, 1)$ yields together with (6.1)

$$\begin{aligned} b[(\mathbf{u}, \bar{A}), (\mathbf{u}, \bar{A})] &\geq \lambda \|\operatorname{div}(\mathbf{u})\|^2 + 2\mu L_c^2 \|D\bar{A}\|^2 \\ &\quad + 2\mu_c(1 - \alpha) \|\operatorname{skew}(D\mathbf{u})\|^2 + 2\mu_c \left(1 - \frac{1}{\alpha}\right) \|\bar{A}\|^2 \\ &\geq \lambda \|\operatorname{div}(\mathbf{u})\|^2 + \mu L_c^2 \|D\bar{A}\|^2 \\ &\quad + 2\mu_c(1 - \alpha) \|\operatorname{skew}(D\mathbf{u})\|^2 + \left(2\mu_c \left(1 - \frac{1}{\alpha}\right) + \frac{\mu L_c^2}{C_1^2}\right) \|\bar{A}\|^2, \end{aligned}$$

which gives for $1 > \alpha > \frac{\mu_c}{\mu + \frac{\mu L_c^2}{C_1^2}} \geq \frac{\mu_c}{\mu_c + \frac{\mu L_c^2}{C_1^2}}$ and $\mu_c \in (0, \mu]$

$$b[(\mathbf{u}, \bar{A}), (\mathbf{u}, \bar{A})] \geq 4\mu_c c_4 \left(\|D\mathbf{u}\|^2 + \|D\bar{A}\|^2 \right)$$

using (6.3), where c_4 depends on λ, μ and L_c but c_4 is independent of μ_c . Thus, $I_{\text{incr}}^n(\cdot)$ is uniformly convex since $\psi_{\mathbf{K}}(\cdot)$ is convex, $b[\cdot, \cdot]$ is coercive and $\ell^n[\cdot]$ is linear. Finally, we obtain the assertion from $\psi_{\mathbf{K}} \geq 0$ and

$$\begin{aligned} I_{\text{incr}}^n(\mathbf{u}, \bar{A}) &\geq \frac{1}{2} b[(\mathbf{u}, \bar{A}), (\mathbf{u}, \bar{A})] - \ell^n(\mathbf{u}) \\ &\geq 2\mu_c c_4 \left(\|D\mathbf{v}\|^2 + \|D\bar{A}\|^2 \right) - \frac{1}{4\mu_c c_4} \|\ell^n\|_{\mathbf{V}'}^2 - \mu_c c_4 \|D\mathbf{u}\|^2. \quad \square \end{aligned}$$

In the pure Dirichlet case this gives directly for the norm

$$\|(\mathbf{u}, \bar{A})\|_{\mathbf{V} \times W} = \left(\|D\mathbf{u}\|^2 + \|D\bar{A}\|^2 \right)^{1/2}$$

the following *a priori* bound for the solution.

Corollary 6.1. *The minimization problem (5.3) has a unique solution $(\mathbf{u}_h^n, \bar{A}_h^n) \in \mathbf{V}_h \times W_h$ of the discrete incremental problem, which is uniquely characterized by the nonlinear variational problem (5.2), i.e.*

$$DI_{\text{incr}}^n(\mathbf{u}_h^n, \bar{A}_h^n)[\mathbf{v}_h, \bar{B}_h] = 0, \quad (\mathbf{v}_h, \bar{B}_h) \in \mathbf{V}_h \times W_h, \tag{6.5}$$

and which solves the discrete system (3.5). Moreover, we have the a priori bound

$$\|(\mathbf{u}_h, \bar{A}_h)\|_{\mathbf{V} \times W}^2 \leq \frac{2}{\mu_c C_4} \left(\|\ell^n\|_{\mathbf{V}'}^2 + 2\mu \|\varepsilon_p^{n-1}\|^2 \right). \tag{6.6}$$

Analogously, a unique solution $(\mathbf{u}^n, \bar{A}^n) \in \mathbf{V} \times W$ of the incremental problem in the continuous spaces exists, satisfying

$$DI_{\text{incr}}^n(\mathbf{u}^n, \bar{A}^n)[\mathbf{v}, \bar{B}] = 0, \quad (\mathbf{v}, \bar{B}) \in \mathbf{V} \times W. \tag{6.7}$$

Theorem 6.2. *We have*

$$\|(\mathbf{u} - \mathbf{u}_h, \bar{A} - \bar{A}_h)\|_{\mathbf{V} \times W} \leq \frac{C_5}{\mu_c} \inf_{(\mathbf{v}_h, \bar{B}_h) \in \mathbf{V}_h \times W_h} \|(\mathbf{u} - \mathbf{v}_h, \bar{A} - \bar{B}_h)\|_{\mathbf{V} \times W}. \tag{6.8}$$

Again C_5 is independent of $\mu_c \in (0, \mu]$.

Proof. Since the projection $P_{\mathbf{K}}$ is non-expansive, the derivative $DI_{\text{incr}}^n(\cdot)$ is uniformly Lipschitz continuous satisfying

$$\|DI_{\text{incr}}^n(\mathbf{u}, \bar{A}) - DI_{\text{incr}}^n(\mathbf{v}, \bar{B})\|_{\mathbf{V} \times W} \leq C_6 \|(\mathbf{u}, \bar{A}) - (\mathbf{v}, \bar{B})\|_{\mathbf{V} \times W} \tag{6.9}$$

with $C_6 > 0$ independent of $\mu_c \in (0, \mu]$. Since $I_{\text{incr}}^n(\cdot)$ is uniformly convex and inserting (6.5), (6.7), (6.9) gives

$$\begin{aligned} & \mu_c C_4 \|(\mathbf{u}^n - \mathbf{u}_h^n, \bar{A}^n - \bar{A}_h^n)\|_{\mathbf{V} \times W}^2 \\ & \leq DI_{\text{incr}}^n(\mathbf{u}^n, \bar{A}^n)[\mathbf{u}^n - \mathbf{u}_h^n, \bar{A}^n - \bar{A}_h^n] - DI_{\text{incr}}^n(\mathbf{u}_h^n, \bar{A}_h^n)[\mathbf{u}^n - \mathbf{u}_h^n, \bar{A}^n - \bar{A}_h^n] \\ & = -DI_{\text{incr}}^n(\mathbf{u}_h^n, \bar{A}_h^n)[\mathbf{u}^n - \mathbf{v}_h, \bar{A}^n - \bar{B}_h] \\ & = DI_{\text{incr}}^n(\mathbf{u}^n, \bar{A}^n)[\mathbf{u}^n - \mathbf{v}_h, \bar{A}^n - \bar{B}_h] - DI_{\text{incr}}^n(\mathbf{u}_h^n, \bar{A}_h^n)[\mathbf{u}^n - \mathbf{v}_h, \bar{A}^n - \bar{B}_h] \\ & \leq \|DI_{\text{incr}}^n(\mathbf{u}^n, \bar{A}^n) - DI_{\text{incr}}^n(\mathbf{u}_h^n, \bar{A}_h^n)\|_{\mathbf{V} \times W} \|(\mathbf{u}^n - \mathbf{v}_h, \bar{A}^n - \bar{B}_h)\|_{\mathbf{V} \times W} \\ & \leq C_6 \|(\mathbf{u}^n - \mathbf{u}_h^n, \bar{A}^n - \bar{A}_h^n)\|_{\mathbf{V} \times W} \|(\mathbf{u}^n - \mathbf{v}_h, \bar{A}^n - \bar{B}_h)\|_{\mathbf{V} \times W}. \quad \square \end{aligned}$$

Remark 6.1. Here, we do not discuss the convergence in time. Formally, the problem has the same structure as considered in Ref. 34 for the generalized stresses in the case of plasticity with hardening. Thus, we expect also first order convergence in $\Delta t \rightarrow 0$ for the implicit Euler method. Our numerical experiments show that for realistic time step sizes the spatial error is dominant and therefore there is no need for higher order methods in time.

7. The Dual Problem of the Elasto-Plastic Cosserat Model

The uniform convexity and the finite element convergence estimate derived in the previous section deteriorate in the limit $\mu_c \rightarrow 0$. This reflects the missing regularity of the primal solution of the limiting model of perfect plasticity. Thus, in this section we derive the dual formulation in order to study the dependence of the solution on μ_c . For simplicity, we study $d = 3$.

Let $(\mathbf{u}^n, \bar{A}^n, \boldsymbol{\sigma}^n)$ be the solution of the incremental problem. From (3.5c) and (3.5d) we obtain $\text{skew}(\boldsymbol{\sigma}^n) = 2\mu_c(\text{skew}(D\mathbf{u}^n) - \bar{A}^n)$ and $\int_{\Omega} \boldsymbol{\sigma}^n : D\mathbf{u}^n \, d\mathbf{x} = \ell^n[\mathbf{u}^n]$. Now, (3.5e) and

$$\begin{aligned} & \int_{\Omega} \text{skew}(\boldsymbol{\sigma}^n) : D\mathbf{u}^n \, d\mathbf{x} \\ &= \int_{\Omega} \text{skew}(\boldsymbol{\sigma}^n) : (\text{skew}(D\mathbf{u}^n) - \bar{A}^n) \, d\mathbf{x} + \int_{\Omega} \text{skew}(\boldsymbol{\sigma}^n) : \bar{A}^n \, d\mathbf{x} \\ &= 2\mu_c \int_{\Omega} |\text{skew}(D\mathbf{u}^n) - \bar{A}^n|^2 \, d\mathbf{x} + 2\mu L_c^2 \int_{\Omega} |D\bar{A}^n|^2 \, d\mathbf{x} \end{aligned}$$

yields for the primal functional (5.3)

$$\begin{aligned} I_{\text{incr}}^n(\mathbf{u}^n, \bar{A}^n) &= \mathcal{E}_{\text{incr}}(D\mathbf{u}^n, \bar{A}^n, \boldsymbol{\varepsilon}_p^{n-1}) - \ell^n[\mathbf{u}^n] \\ &= \frac{1}{2\mu} \int_{\Omega} \psi_{\mathbf{K}}(\boldsymbol{\theta}^n) \, d\mathbf{x} + \frac{\lambda}{2} \int_{\Omega} \text{tr}(D\mathbf{u}^n)^2 \, d\mathbf{x} \\ &\quad + \mu_c \int_{\Omega} |\text{skew}(D\mathbf{u}^n) - \bar{A}^n|^2 \, d\mathbf{x} + \mu L_c^2 \int_{\Omega} |D\bar{A}^n|^2 \, d\mathbf{x} - \ell^n[\mathbf{u}^n] \\ &= \frac{1}{2\mu} \int_{\Omega} \psi_{\mathbf{K}}(\boldsymbol{\theta}^n) \, d\mathbf{x} + \frac{\lambda}{2} \int_{\Omega} \text{tr}(D\mathbf{u}^n)^2 \, d\mathbf{x} \\ &\quad + \frac{1}{2} \int_{\Omega} \text{skew}(\boldsymbol{\sigma}^n) : D\mathbf{u}^n \, d\mathbf{x} - \int_{\Omega} \boldsymbol{\sigma}^n : D\mathbf{u}^n \, d\mathbf{x} \\ &= \frac{1}{2\mu} \int_{\Omega} \psi_{\mathbf{K}}(\boldsymbol{\theta}^n) \, d\mathbf{x} + \frac{\lambda}{2} \int_{\Omega} \text{tr}(D\mathbf{u}^n)^2 \, d\mathbf{x} \\ &\quad - \frac{1}{2} \int_{\Omega} \text{skew}(\boldsymbol{\sigma}^n) : D\mathbf{u}^n \, d\mathbf{x} - \int_{\Omega} \text{sym}(\boldsymbol{\sigma}^n) : D\mathbf{u}^n \, d\mathbf{x}. \end{aligned}$$

Again using (5.1) and (5.3) we obtain

$$\begin{aligned} \text{sym}(\boldsymbol{\sigma}^n) &= P_{\mathbf{K}}(\boldsymbol{\theta}^n) + \lambda \text{div}(\mathbf{u}^n) \mathbf{1}, \\ \text{dev}(\text{sym}(\boldsymbol{\sigma}^n)) &= \text{dev}(P_{\mathbf{K}}(\boldsymbol{\theta}^n)), \\ P_{\mathbf{K}}(\boldsymbol{\theta}^n) &= \text{dev}(\text{sym}(\boldsymbol{\sigma}^n)) + \frac{2\mu}{3} \text{tr}(D\mathbf{u}^n) \mathbf{1}, \\ \psi_{\mathbf{K}}(\boldsymbol{\theta}^n) &= \frac{1}{2} |\boldsymbol{\theta}^n|^2 - \frac{1}{2} |\boldsymbol{\theta}^n - P_{\mathbf{K}}(\boldsymbol{\theta}^n)|^2 = P_{\mathbf{K}}(\boldsymbol{\theta}^n) : \boldsymbol{\theta}^n - \frac{1}{2} |P_{\mathbf{K}}(\boldsymbol{\theta}^n)|^2 \\ &= 2\mu \text{dev}(\text{sym}(\boldsymbol{\sigma}^n)) : (D\mathbf{u}^n - \boldsymbol{\varepsilon}_p^{n-1}) \end{aligned}$$

$$\begin{aligned} & + \frac{2\mu^2}{3} \operatorname{tr}(D\mathbf{u}^n)^2 - \frac{1}{2} |\operatorname{dev}(\operatorname{sym}(\boldsymbol{\sigma}^n))|^2, \\ \operatorname{tr}(\boldsymbol{\sigma}^n)\mathbb{1} : D\mathbf{u}^n & = \frac{1}{2\mu + 3\lambda} \operatorname{tr}(\boldsymbol{\sigma}^n)^2 = (2\mu + 3\lambda) \operatorname{tr}(D\mathbf{u}^n)^2, \end{aligned}$$

and together with

$$\int_{\Omega} \operatorname{skew}(\boldsymbol{\sigma}^n) : D\mathbf{u}^n \, d\mathbf{x} = \frac{1}{2\mu_c} \int_{\Omega} \operatorname{skew}(\boldsymbol{\sigma}^n) : \operatorname{skew}(\boldsymbol{\sigma}^n) \, d\mathbf{x} + 2\mu L_c^2 \int_{\Omega} D\bar{A}^n \cdot D\bar{A}^n \, d\mathbf{x},$$

we finally obtain

$$\begin{aligned} I_{\text{incr}}^n(\mathbf{u}^n, \bar{A}^n) & = \frac{1}{2\mu} \int_{\Omega} \psi_{\mathbf{K}}(\boldsymbol{\theta}^n) \, d\mathbf{x} + \frac{\lambda}{2} \int_{\Omega} \operatorname{tr}(D\mathbf{u}^n)^2 \, d\mathbf{x} \\ & \quad - \frac{1}{2} \int_{\Omega} \operatorname{skew}(\boldsymbol{\sigma}^n) : D\mathbf{u}^n \, d\mathbf{x} - \int_{\Omega} \operatorname{sym}(\boldsymbol{\sigma}^n) : D\mathbf{u}^n \, d\mathbf{x} \\ & = \int_{\Omega} \operatorname{dev}(\operatorname{sym}(\boldsymbol{\sigma}^n)) : (D\mathbf{u}^n - \boldsymbol{\varepsilon}_p^{n-1}) \, d\mathbf{x} + \frac{2\mu + 3\lambda}{6} \int_{\Omega} \operatorname{tr}(D\mathbf{u}^n)^2 \, d\mathbf{x} \\ & \quad - \frac{1}{4\mu} \int_{\Omega} |\operatorname{dev}(\operatorname{sym}(\boldsymbol{\sigma}^n))|^2 \, d\mathbf{x} - \frac{1}{2} \int_{\Omega} \operatorname{skew}(\boldsymbol{\sigma}^n) : D\mathbf{u}^n \, d\mathbf{x} \\ & \quad - \int_{\Omega} \operatorname{sym}(\boldsymbol{\sigma}^n) : D\mathbf{u}^n \, d\mathbf{x} \\ & = - \int_{\Omega} \boldsymbol{\sigma}^n : \boldsymbol{\varepsilon}_p^{n-1} \, d\mathbf{x} - \frac{1}{4\mu} \int_{\Omega} |\operatorname{dev}(\operatorname{sym}(\boldsymbol{\sigma}^n))|^2 \, d\mathbf{x} + \frac{1}{6} \int_{\Omega} \operatorname{tr}(\boldsymbol{\sigma}^n)\mathbb{1} : D\mathbf{u}^n \, d\mathbf{x} \\ & \quad - \frac{1}{2} \int_{\Omega} \operatorname{skew}(\boldsymbol{\sigma}^n) : D\mathbf{u}^n \, d\mathbf{x} - \frac{1}{3} \int_{\Omega} \operatorname{tr}(\boldsymbol{\sigma}^n)\mathbb{1} : D\mathbf{u}^n \, d\mathbf{x} \\ & = - \int_{\Omega} \boldsymbol{\sigma}^n : \boldsymbol{\varepsilon}_p^{n-1} \, d\mathbf{x} - \frac{1}{4\mu} \int_{\Omega} |\operatorname{dev}(\operatorname{sym}(\boldsymbol{\sigma}^n))|^2 \, d\mathbf{x} - \frac{1}{6(2\mu + 3\lambda)} \int_{\Omega} \operatorname{tr}(\boldsymbol{\sigma}^n)^2 \, d\mathbf{x} \\ & \quad - \frac{1}{4\mu_c} \int_{\Omega} |\operatorname{skew}(\boldsymbol{\sigma}^n)|^2 \, d\mathbf{x} - \mu L_c^2 \int_{\Omega} |D\bar{A}^n|^2 \, d\mathbf{x}. \end{aligned}$$

Thus, we define the *dual functional*

$$\begin{aligned} \mathcal{D}_{\text{incr}}^n(\boldsymbol{\sigma}, \bar{A}) & = \int_{\Omega} \boldsymbol{\sigma} : \boldsymbol{\varepsilon}_p^{n-1} \, d\mathbf{x} + \frac{1}{4\mu} \int_{\Omega} |\operatorname{dev}(\operatorname{sym}(\boldsymbol{\sigma}))|^2 \, d\mathbf{x} + \frac{1}{6(2\mu + 3\lambda)} \int_{\Omega} \operatorname{tr}(\boldsymbol{\sigma})^2 \, d\mathbf{x} \\ & \quad + \frac{1}{4\mu_c} \int_{\Omega} |\operatorname{skew}(\boldsymbol{\sigma})|^2 \, d\mathbf{x} + \mu L_c^2 \int_{\Omega} |D\bar{A}|^2 \, d\mathbf{x}. \end{aligned} \tag{7.1}$$

Standard calculus in convex analysis yields the following lemma.

Lemma 7.1. *Let $\boldsymbol{\varepsilon}_p^{n-1} \in L_2(\Omega, \operatorname{Sym}(3))$ with $\operatorname{tr}(\boldsymbol{\varepsilon}_p^{n-1}) = 0$ be given. Then, $(\boldsymbol{\sigma}^n, \bar{A}^n) \in L_2(\Omega, \mathbb{R}^{3,3}) \times W$ is uniquely determined by minimizing the dual*

functional (7.1) subject to the plastic constraint

$$\phi(\text{sym}(\boldsymbol{\sigma}^n)) \leq 0 \tag{7.2}$$

and the equilibrium constraint

$$\int_{\Omega} \boldsymbol{\sigma}^n : D\mathbf{v} \, d\mathbf{x} = \ell^n[\mathbf{v}], \quad \mathbf{v} \in \mathbf{V}, \tag{7.3}$$

$$2\mu L_c^2 \int_{\Omega} D\bar{A}^n \cdot D\bar{B} \, d\mathbf{x} = \int_{\Omega} \text{skew}(\boldsymbol{\sigma}^n) : \bar{B} \, d\mathbf{x}, \quad \bar{B} \in W. \tag{7.4}$$

From Theorem 6.1 we obtain that for $\mu_c > 0$, a primal solution always exists and therefore a dual solution also exists. For the limit case $\mu_c = 0$, we have to assume that the convex set

$$\mathbf{K}^n = \left\{ \boldsymbol{\tau} \in L^2(\Omega, \text{Sym}(3)) : \boldsymbol{\tau} \in \mathbf{K} \text{ a.e. in } \Omega, \int_{\Omega} \boldsymbol{\tau} : D\mathbf{v} \, d\mathbf{x} = \ell^n[\mathbf{v}], \mathbf{v} \in \mathbf{V} \right\}$$

is not empty (weak safe-load assumption).

Lemma 7.2. *If $\boldsymbol{\eta}^n \in \mathbf{K}^n$ exists, we have*

$$\| \text{skew}(\boldsymbol{\sigma}^n) \|^2 \leq 4\mu_c \mathcal{D}_{\text{incr}}^n(\boldsymbol{\eta}^n, \mathbf{0}) \tag{7.5}$$

and

$$\| D\bar{A}^n \|^2 \leq \frac{C_1^2}{\mu^2 L_c^4} \mu_c \mathcal{D}_{\text{incr}}^n(\boldsymbol{\eta}^n, \mathbf{0}). \tag{7.6}$$

Proof. Since $(\boldsymbol{\eta}^n, \mathbf{0})$ is admissible, we obtain the first assertion from

$$D_{\text{incr}}^n(\boldsymbol{\eta}^n, \mathbf{0}) \geq D_{\text{incr}}^n(\boldsymbol{\sigma}^n, \bar{A}^n) = D_{\text{incr}}^n(\text{sym}(\boldsymbol{\sigma}^n), \bar{A}^n) + \frac{1}{4\mu_c} \int_{\Omega} | \text{skew}(\boldsymbol{\sigma}^n) |^2 \, d\mathbf{x} \tag{7.7}$$

since $D_{\text{incr}}^n(\text{sym}(\boldsymbol{\sigma}^n), \bar{A}^n) \geq 0$. Testing with $\bar{B} = \bar{A}^n$ we obtain from (7.4)

$$2\mu L_c^2 \| D\bar{A}^n \|^2 \leq \| \text{skew}(\boldsymbol{\sigma}^n) \| \| \bar{A}^n \| \leq C_1 \| \text{skew}(\boldsymbol{\sigma}^n) \| \| D\bar{A}^n \|,$$

where the second inequality follows from (6.1). This gives directly the second assertion by inserting the first statement. □

Now, we denote the incremental dual solution for fixed $\boldsymbol{\varepsilon}_p^{n-1} \in L_2(\Omega, \text{Sym}(3))$ by $(\boldsymbol{\sigma}_{\mu_c}^n, \bar{A}_{\mu_c}^n)$.

If $\mathbf{K}^n \neq \emptyset$, a unique dual solution of perfect plasticity $\boldsymbol{\sigma}_0^n \in \mathbf{K}^n$ defined by

$$\mathcal{D}_{\text{incr}}^n(\boldsymbol{\sigma}_0^n, \mathbf{0}) \leq \mathcal{D}_{\text{incr}}^n(\boldsymbol{\tau}, \mathbf{0}), \quad \boldsymbol{\tau} \in \mathbf{K}^n$$

exists.⁶⁹ Equivalently, $\boldsymbol{\sigma}_0^n \in \mathbf{K}^n$ is characterized by

$$d[\boldsymbol{\sigma}_0^n, \boldsymbol{\sigma}_0^n - \boldsymbol{\tau}] \leq \int_{\Omega} (\boldsymbol{\sigma}_0^n - \boldsymbol{\tau}) : \boldsymbol{\varepsilon}_p^{n-1} \, d\mathbf{x}, \quad \boldsymbol{\tau} \in \mathbf{K}^n \tag{7.8}$$

with the symmetric bilinear form

$$d[\boldsymbol{\sigma}, \boldsymbol{\tau}] = \frac{1}{2\mu} \int_{\Omega} \text{dev}(\text{sym}(\boldsymbol{\sigma})) : \text{dev}(\text{sym}(\boldsymbol{\tau})) \, d\mathbf{x} + \frac{1}{6(2\mu + 3\lambda)} \int_{\Omega} \text{tr}(\boldsymbol{\sigma}) \text{tr}(\boldsymbol{\tau}) \, d\mathbf{x}.$$

Now, we study the limit $\mu_c \rightarrow 0$.

Theorem 7.1. *If $\boldsymbol{\eta}^n \in \mathbf{K}^n$ exists, we have*

$$\lim_{\mu_c \rightarrow 0} \|\text{sym}(\boldsymbol{\sigma}_{\mu_c}^n) - \boldsymbol{\sigma}_0^n\| = 0. \tag{7.9}$$

Proof. The proof follows the general framework of penalty solutions of variational inequalities.²⁹

Let μ_c^j be a decreasing sequence with $\mu_c^j \rightarrow 0$. Since $\text{sym}(\boldsymbol{\sigma}_{\mu_c^j}^n)$ is uniformly bounded by (7.7), we can extract a subsequence (again denoted by $\text{sym}(\boldsymbol{\sigma}_{\mu_c^j}^n)$) which is weakly convergent to $\hat{\boldsymbol{\sigma}}^n \in L^2(\Omega, \text{Sym}(3))$. We have $\boldsymbol{\sigma}_{\mu_c^j}^n \in \mathbf{K}$ and therefore $\hat{\boldsymbol{\sigma}}^n \in \mathbf{K}$ a.e. in Ω . Moreover, for $\mathbf{v} \in \mathbf{V}$ we obtain from (7.3) and (7.5)

$$\begin{aligned} \int_{\Omega} \hat{\boldsymbol{\sigma}}^n : D\mathbf{v} \, d\mathbf{x} - \ell^n[\mathbf{v}] &= \lim_{j \rightarrow \infty} \int_{\Omega} \text{sym}(\boldsymbol{\sigma}_{\mu_c^j}^n) : D\mathbf{v} \, d\mathbf{x} - \ell^n[\mathbf{v}] \\ &= \lim_{j \rightarrow \infty} \int_{\Omega} \text{skew}(\boldsymbol{\sigma}_{\mu_c^j}^n) : D\mathbf{v} = 0. \end{aligned}$$

Thus, we have $\hat{\boldsymbol{\sigma}}^n \in \mathbf{K}^n$.

For all $\boldsymbol{\tau} \in \mathbf{K}^n$ the pair $(\boldsymbol{\tau}, \mathbf{0})$ is admissible for the incremental dual Cosserat problem satisfying (7.3), (7.4), which gives

$$\begin{aligned} d[\text{sym}(\boldsymbol{\sigma}_{\mu_c^j}^n), \text{sym}(\boldsymbol{\sigma}_{\mu_c^j}^n) - \boldsymbol{\tau}] &+ \frac{1}{2\mu_c} \int_{\Omega} |\text{skew}(\boldsymbol{\sigma}_{\mu_c^j}^n)|^2 \, d\mathbf{x} + 2\mu L_c^2 \int_{\Omega} |D\bar{A}_{\mu_c^j}^n|^2 \, d\mathbf{x} \\ &\leq \int_{\Omega} (\boldsymbol{\sigma}_{\mu_c^j}^n - \boldsymbol{\tau}) : \boldsymbol{\varepsilon}_p^{n-1} \, d\mathbf{x}. \end{aligned} \tag{7.10}$$

Passing to the limit yields

$$d[\hat{\boldsymbol{\sigma}}^n, \hat{\boldsymbol{\sigma}}^n] \leq \liminf_{j \rightarrow \infty} d[\text{sym}(\boldsymbol{\sigma}_{\mu_c^j}^n), \text{sym}(\boldsymbol{\sigma}_{\mu_c^j}^n)] \leq d[\hat{\boldsymbol{\sigma}}^n, \boldsymbol{\tau}] + \int_{\Omega} (\hat{\boldsymbol{\sigma}}^n - \boldsymbol{\tau}) : \boldsymbol{\varepsilon}_p^{n-1} \, d\mathbf{x}.$$

Since $\boldsymbol{\sigma}_0^n \in \mathbf{K}^n$ is uniquely characterized by (7.8), this proves that the weak limit solves the dual problem of perfect plasticity, i.e. $\hat{\boldsymbol{\sigma}}^n = \boldsymbol{\sigma}_0^n$.

Finally, we show strong convergence. Inserting $\boldsymbol{\tau} = \boldsymbol{\sigma}_0^n$ in (7.10) gives

$$d[\text{sym}(\boldsymbol{\sigma}_{\mu_c^j}^n), \text{sym}(\boldsymbol{\sigma}_{\mu_c^j}^n)] \leq d[\text{sym}(\boldsymbol{\sigma}_{\mu_c^j}^n), \boldsymbol{\sigma}_0^n] + \int_{\Omega} (\boldsymbol{\sigma}_{\mu_c^j}^n - \boldsymbol{\sigma}_0^n) : \boldsymbol{\varepsilon}_p^{n-1} \, d\mathbf{x},$$

which gives

$$\begin{aligned} &d[\text{sym}(\boldsymbol{\sigma}_{\mu_c^j}^n) - \boldsymbol{\sigma}_0^n, \text{sym}(\boldsymbol{\sigma}_{\mu_c^j}^n) - \boldsymbol{\sigma}_0^n] \\ &= d[\text{sym}(\boldsymbol{\sigma}_{\mu_c^j}^n), \text{sym}(\boldsymbol{\sigma}_{\mu_c^j}^n)] - d[\text{sym}(\boldsymbol{\sigma}_{\mu_c^j}^n), \boldsymbol{\sigma}_0^n] - d[\boldsymbol{\sigma}_0^n, \text{sym}(\boldsymbol{\sigma}_{\mu_c^j}^n)] + d[\boldsymbol{\sigma}_0^n, \boldsymbol{\sigma}_0^n] \\ &\leq d[\text{sym}(\boldsymbol{\sigma}_{\mu_c^j}^n), \boldsymbol{\sigma}_0^n] + \int_{\Omega} (\boldsymbol{\sigma}_{\mu_c^j}^n - \boldsymbol{\sigma}_0^n) : \boldsymbol{\varepsilon}_p^{n-1} \, d\mathbf{x} \\ &\quad - d[\text{sym}(\boldsymbol{\sigma}_{\mu_c^j}^n), \boldsymbol{\sigma}_0^n] - d[\boldsymbol{\sigma}_0^n, \text{sym}(\boldsymbol{\sigma}_{\mu_c^j}^n)] + d[\boldsymbol{\sigma}_0^n, \boldsymbol{\sigma}_0^n]. \end{aligned}$$

The limit on the right-hand side is well defined, and we obtain

$$\lim_{j \rightarrow \infty} d \left[\text{sym}(\boldsymbol{\sigma}_{\mu_c^j}^n) - \boldsymbol{\sigma}_0^n, \text{sym}(\boldsymbol{\sigma}_{\mu_c^j}^n) - \boldsymbol{\sigma}_0^n \right] = 0.$$

This proves the assertion since $d[\cdot, \cdot]$ is an inner product in $L_2(\Omega, \text{Sym}(3))$. □

Remark 7.1. Our numerical experiments suggest that we have

$$\| \text{sym}(\boldsymbol{\sigma}_{\mu_c}^n) - \boldsymbol{\sigma}_0^n \| = O(\sqrt{\mu_c}).$$

We surmise that in general, additional regularity assumptions are required to obtain an explicit estimate of this type. In principle, such an estimate could then be used for estimating perfect plasticity in the form

$$\begin{aligned} \| \boldsymbol{\sigma}_0 - \boldsymbol{\sigma}_{0,h} \| &\leq \| \boldsymbol{\sigma}_0 - \text{sym}(\boldsymbol{\sigma}_{\mu_c}) \| + \| \text{sym}(\boldsymbol{\sigma}_{\mu_c}) - \text{sym}(\boldsymbol{\sigma}_{\mu_c,h}) \| \\ &\quad + \| \text{sym}(\boldsymbol{\sigma}_{\mu_c,h}) - \boldsymbol{\sigma}_{0,h} \| \end{aligned}$$

by a suitable choice of $\mu_c = \mu_c(h)$. Note that an analogous result is obtained in Ref. 60 for the static case by approximating perfect plasticity with plasticity with hardening for vanishing hardening modulus. It is not clear if such a result can be transferred to the quasi-static case where in general the plastic strain is not smooth enough.

8. Numerical Solution Algorithm

We formulate a semi-smooth Newton method for the nonlinear variational problem

$$(\mathbf{u}^n, \bar{A}^n) \in \mathbf{V}_h(\mathbf{u}_D^n) \times W_h(\bar{A}_D^n): \quad F^n(\mathbf{u}^n, \bar{A}^n) = 0$$

in every time step n , where F^n is the first variation of I_{incr}^n defined by

$$F^n(\mathbf{u}, \bar{A})[\mathbf{v}, \bar{B}] = DI_{\text{incr}}^n(\mathbf{u}, \bar{A})[\mathbf{v}, \bar{B}], \quad (\mathbf{v}, \bar{B}) \in \mathbf{V}_h(\mathbf{0}) \times W_h(\mathbf{0})$$

(cf. Lemma 5.2). The functional F^n is semi-smooth, and the variation $\partial F^n = \partial^2 I_{\text{incr}}^n$ is symmetric and multi-valued. Thus, the corresponding semi-smooth Newton method can be formally written as

$$0 \in F^n(\mathbf{u}^{n,k}, \bar{A}^{n,k}) + \partial F^n(\mathbf{u}^{n,k}, \bar{A}^{n,k})[\mathbf{u}^{n,k+1} - \mathbf{u}^{n,k}, \bar{A}^{n,k+1} - \bar{A}^{n,k}].$$

Since I_{incr}^n is convex and $F^n = DI_{\text{incr}}^n$ is Lipschitz continuous, this can be analyzed within the framework of generalized Newton methods.³⁸

We consider the special case of the von Mises flow rule by inserting (4.5). This results in the following realization of the semi-smooth Newton method.

- (S0) We start for $t_0 = 0$ with $\boldsymbol{\varepsilon}_p^0 = \mathbf{0}$, and we set $n = 1$.
- (S1) Choose $\mathbf{u}^{n,0}$, $\bar{A}^{n,0}$ and set $k = 0$. Then, set Dirichlet boundary values $\mathbf{u}^{n,0}(\mathbf{x}) = \mathbf{u}_D^n(\mathbf{x})$ for all $\mathbf{x} \in D$ and $\bar{A}^{n,0}(\mathbf{x}) = \bar{A}_D^n(\mathbf{x})$ for all $\mathbf{x} \in D'$.

(S2) Compute for every integration point $\boldsymbol{\xi} \in \Xi_h$

$$\begin{aligned} \boldsymbol{\theta}^{n,k}(\boldsymbol{\xi}) &= 2\mu(\text{sym}(D\mathbf{u}^{n,k}(\boldsymbol{\xi})) - \boldsymbol{\varepsilon}_p^{n-1}(\boldsymbol{\xi})), \\ \boldsymbol{\eta}^{n,k}(\boldsymbol{\xi}) &= \frac{\text{dev}(\boldsymbol{\theta}^{n,k}(\boldsymbol{\xi}))}{|\text{dev}(\boldsymbol{\theta}^{n,k}(\boldsymbol{\xi}))|}, \\ T_E^{n,k}(\boldsymbol{\xi}) &= \boldsymbol{\theta}^{n,k}(\boldsymbol{\xi}) - \max\{0, |\text{dev}(\boldsymbol{\theta}^{n,k}(\boldsymbol{\xi}))| - K_0\} \boldsymbol{\eta}^{n,k}(\boldsymbol{\xi}), \\ \boldsymbol{\sigma}^{n,k}(\boldsymbol{\xi}) &= T_E^{n,k}(\boldsymbol{\xi}) + \lambda \text{div}(\mathbf{u}^n)(\boldsymbol{\xi}) \mathbf{1} + 2\mu_c(\text{skew}(D\mathbf{u}^n(\boldsymbol{\xi})) - \bar{A}^n(\boldsymbol{\xi})). \end{aligned}$$

(S3) Compute the residual

$$\begin{aligned} F^{n,k}[\mathbf{v}, \bar{B}] &= \int_{\Omega} \boldsymbol{\sigma}^{n,k} : D\mathbf{v} \, d\mathbf{x} - \ell^n[\mathbf{v}] \\ &\quad + 2\mu L_c^2 \int_{\Omega} D\bar{A}^{n,k} \cdot D\bar{B} \, d\mathbf{x} - 2\mu_c \int_{\Omega} (\text{skew}(D\mathbf{u}^{n,k}) - \bar{A}^{n,k}) : \bar{B} \, d\mathbf{x}. \end{aligned}$$

If $\|F^{n,k}\|$ is small enough, set $\mathbf{u}^n = \mathbf{u}^{n,k}$, $\bar{A}^n = \bar{A}^{n,k}$,

$$\boldsymbol{\varepsilon}_p^n(\boldsymbol{\xi}) = \boldsymbol{\varepsilon}_p^{n-1}(\boldsymbol{\xi}) + \frac{\max\{0, |\text{dev}(\boldsymbol{\theta}^{n,k}(\boldsymbol{\xi}))| - K_0\}}{2\mu} \boldsymbol{\eta}^{n,k}(\boldsymbol{\xi})$$

and go to the next time step $n := n + 1$ in (S1).

(S4) Compute for every integration point $\boldsymbol{\xi} \in \Xi_h$ the consistent linearization $\mathbb{C}^{n,k}(\boldsymbol{\xi}) = \text{Id}$ for $|\text{dev}(\boldsymbol{\theta}^{n,k}(\boldsymbol{\xi}))| \leq K_0$ and

$$\mathbb{C}^{n,k}(\boldsymbol{\xi}) = \frac{1}{d} \mathbf{1} \otimes \mathbf{1} + \frac{K_0}{|\text{dev}(\boldsymbol{\theta}^{n,k}(\boldsymbol{\xi}))|} \left(\left(\text{Id} - \frac{1}{d} \mathbf{1} \otimes \mathbf{1} \right) - \boldsymbol{\eta}^{n,k}(\boldsymbol{\xi}) \otimes \boldsymbol{\eta}^{n,k}(\boldsymbol{\xi}) \right)$$

for $|\text{dev}(\boldsymbol{\theta}^{n,k}(\boldsymbol{\xi}))| > K_0$, and define the bilinear form

$$\begin{aligned} a^{n,k}[(\mathbf{w}, \bar{C}), (\mathbf{v}, \bar{B})] &= 2\mu \int_{\Omega} \text{sym}(D\mathbf{w}) : \mathbb{C}^{n,k} : \text{sym}(D\mathbf{v}) \, d\mathbf{x} \\ &\quad + \lambda \int_{\Omega} \text{div}(\mathbf{w}) \text{div}(\mathbf{v}) \, d\mathbf{x} \\ &\quad + 2\mu_c \int_{\Omega} (\text{skew}(D\mathbf{w}) - \bar{C}) : (\text{skew}(D\mathbf{v}) - \bar{B}) \, d\mathbf{x} \\ &\quad + 2\mu L_c^2 \int_{\Omega} D\bar{C} \cdot D\bar{B} \, d\mathbf{x}. \end{aligned}$$

(S5) Compute $(\mathbf{w}^{n,k}, \bar{C}^{n,k}) \in \mathbf{V}_h(\mathbf{0}) \times W(\mathbf{0})$ solving the linear variation problem

$$a^{n,k}[(\mathbf{w}^{n,k}, \bar{C}^{n,k}), (\mathbf{v}, \bar{B})] = -F^{n,k}[\mathbf{v}, \bar{B}], \quad (\mathbf{v}, \bar{B}) \in \mathbf{V}_h(\mathbf{0}) \times W_h(\mathbf{0});$$

set $\mathbf{u}^{n,k+1} = \mathbf{u}^{n,k} + \mathbf{w}^{n,k+1}$, $\bar{A}^{n,k+1} = \bar{A}^{n,k} + \bar{C}^{n,k+1}$, and go to the next iteration step $k := k + 1$ in (S2).

In general, we cannot guarantee that the iteration is globally convergent without damping. Therefore, the algorithm can be extended by a time stepping control which adapts the time step such that the nonlinear iteration is convergent within a small number of steps.

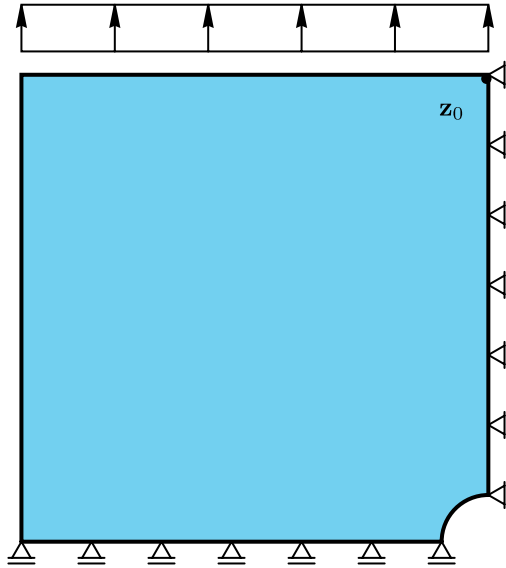


Fig. 1. Geometry and boundary conditions for the test problem. For the numerical comparisons, we evaluate the vertical displacement at the upper right corner $\mathbf{z}_0 = (10, 10)$.

9. Numerical Experiments

In this section we discuss numerical test calculations for the infinitesimal elastoplastic Cosserat model. Therefore, we study a benchmark problem in perfect plasticity.⁴² The computations are realized in the finite element code⁷⁴ M++ supporting parallel multigrid methods.

The geometry and the boundary conditions are illustrated in Fig. 1: let $\Omega = (0, 10) \times (0, 10) \setminus B_1(10, 0)[\text{mm}^2]$ be a quarter of a rectangle with a hole. The Dirichlet data arising by assuming symmetry of the solution are given by

$$\begin{aligned} u_1(10, x_2) &= 0, & A(10, x_2) &= 0, & x_2 \in (1, 10), \\ u_2(x_1, 0) &= 0, & A(x_1, 0) &= 0, & x_1 \in (0, 9). \end{aligned}$$

On the remaining parts of the boundary the microrotations \bar{A} are assumed to satisfy free Neumann boundary conditions in order to minimize the disturbance caused by their presence in the model. The load functional given by

$$\ell(t, \mathbf{v}) = 100 t \int_0^{10} \mathbf{v}(x_1, 10) dx_1$$

depends linearly on the loading parameter $t \geq 0$. Within a plane strain assumption, the displacements are embedded into 3-D by the extension $\mathbf{u} = (u_1, u_2, 0)$, and all material computations are performed in 3-D.

The material parameters for this benchmark are given in Table 1, and for the internal length parameter L_c in the Cosserat model we choose a small value in order to keep the elastic Cosserat effect small.

Table 1. Parameters for the Cosserat model for infinitesimal perfect plasticity with von Mises yield criterion. For various test computations a different Cosserat couple modulus is used. In the algorithms we use the Lamé parameter $\mu = E/(2(1 + \nu))$ and $\lambda = E\nu/((1+\nu)(1-2\nu))$ and the compression modulus $\kappa = \frac{2}{3}\mu + \lambda$.

| | | |
|------------------------------------|---------|--|
| Poisson ratio | ν | 0.29 |
| Young modulus | E | 206900.00 (N/mm ²) |
| Yield stress | K_0 | 450.00 (N/mm ²) |
| Cosserat internal length parameter | L_c | 1/48 (mm) |
| Cosserat couple modulus | μ_c | 0, . . . , 10 μ (N/mm ²) |

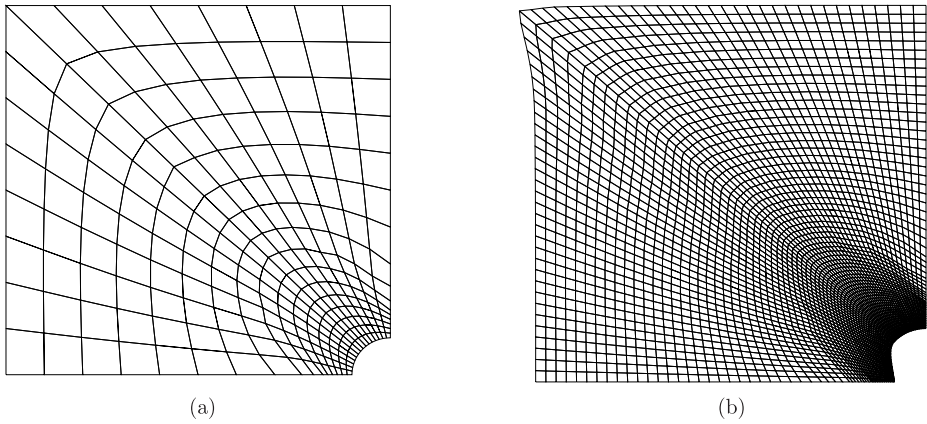


Fig. 2. Coarse mesh (level 0, 256 quadrilaterals) for the benchmark problem (a) and deformed mesh on level 2 (4096 quadrilaterals) for the Cosserat model with $\mu_c = \mu$ at $t = 4.9$ (b).

Table 2. Convergence with respect to the mesh size h for $\mu_c = \mu$ for a fixed time series with $\Delta t_{\max} = 0.25$. The vertical displacement component u_2 is evaluated at the point $\mathbf{z}_0 = (10, 10)^T$ for different loads.

| Level | 1 | 2 | 3 | 4 | 5 | 6 |
|---------------------------|-----------|-----------|-----------|-----------|-----------|-----------|
| Unknowns | 3267 | 12675 | 49923 | 198147 | 789507 | 3151875 |
| h_{\max} | 1.48 | 0.78 | 0.40 | 0.20 | 0.10 | 0.05 |
| $u_2(\mathbf{z}_0, 1)$ | 0.0046533 | 0.0046550 | 0.0046554 | 0.0046555 | 0.0046556 | 0.0046556 |
| $u_2(\mathbf{z}_0, 3)$ | 0.0140210 | 0.0140295 | 0.0140317 | 0.0140324 | 0.0140325 | 0.0140325 |
| $u_2(\mathbf{z}_0, 4)$ | 0.0190866 | 0.0191066 | 0.0191124 | 0.0191138 | 0.0191142 | 0.0191143 |
| $u_2(\mathbf{z}_0, 4.25)$ | 0.0208431 | 0.0208952 | 0.0209105 | 0.0209145 | 0.0209155 | 0.0209158 |
| $u_2(\mathbf{z}_0, 4.5)$ | 0.0240566 | 0.0243134 | 0.0243963 | 0.0244190 | 0.0244249 | 0.0244263 |
| $u_2(\mathbf{z}_0, 4.73)$ | 0.0384216 | 0.0514969 | 0.0723472 | 0.0944045 | 0.1075278 | 0.1123997 |

For simplicity, we use bilinear finite elements on quadrilaterals which are suitable for the application of Theorem 6.2. Note that the approximation can be improved by using more advanced finite elements.^{8,6} The coarse mesh on level 0 (cf. Fig. 2) is refined uniformly. For the numerical results we use up to 3,151,875 unknowns on refinement level 6. In Tables 2 and 3 we test the convergence of the discrete model

Table 3. Convergence in h and Δt_{\max} for $\mu_c = \mu$ and $t = 4.5$. By comparing the convergence rate in time and space we conclude that the error in space is dominating. Moreover, comparing with the results in Table 2 we observe that the results on level 4 are correct up to four digits.

| Level | 2 | 3 | 4 | 5 |
|----------------------------|-----------|-----------|-----------|-----------|
| $\Delta t_{\max} = 1.0$ | 0.0243135 | 0.0243963 | 0.0244190 | 0.0244249 |
| $\Delta t_{\max} = 0.5$ | 0.0243135 | 0.0243963 | 0.0244190 | 0.0244249 |
| $\Delta t_{\max} = 0.25$ | 0.0243134 | 0.0243963 | 0.0244190 | 0.0244249 |
| $\Delta t_{\max} = 0.125$ | 0.0243134 | 0.0243962 | 0.0244189 | 0.0244248 |
| $\Delta t_{\max} = 0.0625$ | 0.0243132 | 0.0243960 | 0.0244187 | 0.0244246 |

Table 4. Convergence for $\mu_c \rightarrow 0$ the displacement evaluated at the point $\mathbf{z}_0 = (10, 10)^T$ with $\Delta t_{\max} = 0.0625$ on level 4. For small values of μ_c we observe linear convergence of the Cosserat model to perfect plasticity.

| μ_c/μ | $u_2(\mathbf{z}_0, 1)$ | $u_2(\mathbf{z}_0, 3)$ | $u_2(\mathbf{z}_0, 4)$ | $u_2(\mathbf{z}_0, 4.4)$ | $u_2(\mathbf{z}_0, 4.6)$ |
|-------------|------------------------|------------------------|------------------------|--------------------------|--------------------------|
| 1 | 0.004655 | 0.014032 | 0.019113 | 0.022586 | 0.028123 |
| 0.1 | 0.004655 | 0.014032 | 0.019114 | 0.022592 | 0.028158 |
| 0.01 | 0.004655 | 0.014032 | 0.019117 | 0.022608 | 0.028262 |
| 0.0016 | 0.004655 | 0.014033 | 0.019119 | 0.022633 | 0.028450 |
| 0.0008 | 0.004655 | 0.014033 | 0.019120 | 0.022641 | 0.028527 |
| 0.0004 | 0.004655 | 0.014033 | 0.019120 | 0.022647 | 0.028592 |
| 0.0002 | 0.004655 | 0.014033 | 0.019121 | 0.022652 | 0.028641 |
| 0.0001 | 0.004655 | 0.014033 | 0.019121 | 0.022655 | 0.028673 |
| 0 | 0.004655 | 0.014033 | 0.019121 | 0.022659 | 0.028720 |

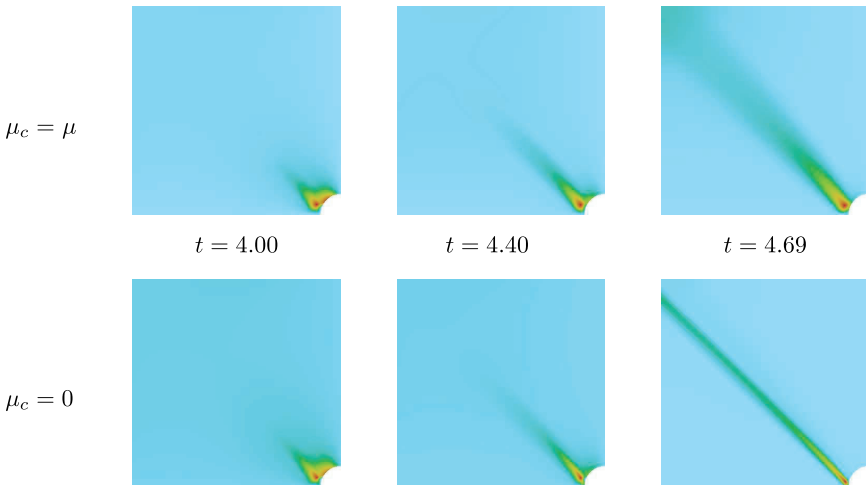


Fig. 3. The distribution of the Cosserat microrotations $|\bar{A}|$ for $\mu_c = \mu$ is compared (on refinement level 4) with the continuum rotations $(1/2)(D_{12}\mathbf{u} - D_{21}\mathbf{u})$ for the model of perfect plasticity ($\mu_c = 0$). Due to the symmetry boundary conditions, the microrotations are zero on the right and the lower boundary.

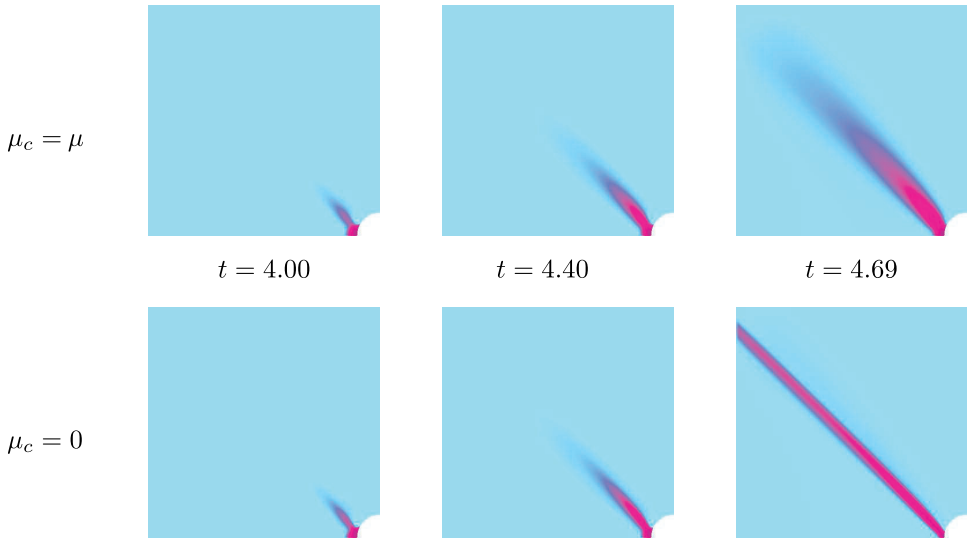


Fig. 4. Distribution of the effective plastic strain for the Cosserat model with $\mu_c = \mu$ and for Prandtl-Reuss ($\mu_c = 0$) on refinement level 4.

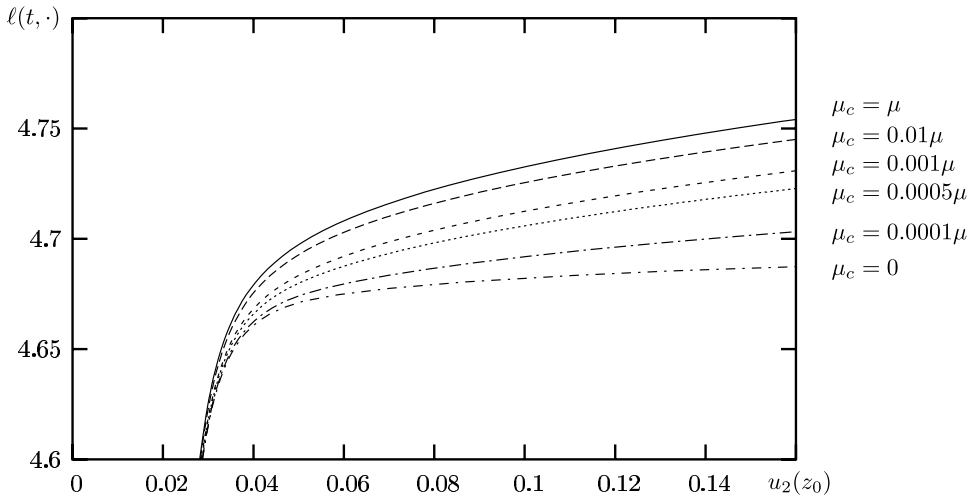


Fig. 5. Load-displacement curve on refinement level 4 for different $\mu_c \in [0, \mu]$. The displacement $\mathbf{u} = (u_1, u_2)$ is evaluated at the point $\mathbf{z}_0 = (10, 10)^T$. For $t < 4.5$ there is nearly no significant difference in the solutions.

with respect to space and time. Results for the deformations, the microrotations, the plastic strain are illustrated in Figs. 2–4.

Finally, we test the limit behavior for $\mu_c \rightarrow 0$. The load displacement curve in Fig. 5 shows the regularization effect of the Cosserat model, and in Table. 4 the convergence to perfect plasticity is tested. The numerical results clearly confirm our theoretical results in Theorem 7.1.

10. Conclusion

Using the Cosserat model as a regularization alternative in problems of mesh-sensitivity of classical Prandtl–Reuss plasticity we have performed a detailed numerical analysis of the corresponding time-incremental problem. Deriving the dual formulation permitted to show analytically convergence of the incremental problem for vanishing Cosserat couple modulus $\mu_c \rightarrow 0$. We have taken great care to track the influence of the appearing material parameters as regards this convergence. Our analytical result is numerically demonstrated for the classical benchmark problem of a plate with a hole in tension. Details of the convergence study are presented.

Acknowledgments

We thank the referees for thoughtful remarks which helped to improve this paper. The second author is supported by Polish grant KBN 1-P03A-031-27.

References

1. E. L. Aero and E. V. Kuvshinskii, Fundamental equations of the theory of elastic media with rotationally interacting particles, *Sov. Phys. Solid State* **2** (1961) 1272–1281.
2. H. D. Alber, *Materials with Memory. Initial–Boundary Value Problems for Constitutive Equations with Internal Variables*, Lecture Notes in Mathematics, Vol. 1682 (Springer, 1998).
3. G. Anzellotti and S. Luckhaus, Dynamical evolution of elasto-perfectly plastic bodies, *Appl. Math. Optim.* **15** (1987) 121–140.
4. J. P. Bardet, Observations on the effects of particle rotations on the failure of idealized granular materials, *Mech. Materials* **18** (1994) 159–182.
5. J. P. Bardet and J. Proubet, A numerical investigation of the structure of persistent shear bands in granular media, *Geotech.* **41** (1991) 599–613.
6. K. J. Bathe, *Finite Element Procedures* (Prentice Hall, 1996).
7. D. Besdo, Ein Beitrag zur nichtlinearen Theorie des Cosserat–Kontinuums, *Acta Mec.* **20** (1974) 105–131.
8. F. Brezzi and M. Fortin, *Mixed and Hybrid Finite Element Methods* (Springer-Verlag, 1991).
9. G. Capriz, *Continua with Microstructure* (Springer, 1989).
10. K. Chelmiński, Coercive approximation of viscoplasticity and plasticity, *Asympt. Anal.* **26** (2001) 105–133.
11. K. Chelmiński, Perfect plasticity as a zero relaxation limit of plasticity with isotropic hardening, *Math. Meth. Appl. Sci.* **24** (2001) 117–136.
12. K. Chelmiński, Global existence of weak-type solutions for models of monotone type in the theory of inelastic deformations, *Math. Meth. Appl. Sci.* **25** (2002) 1195–1230.
13. B. D. Coleman and M. L. Hodgdon, On shear bands in ductile materials, *Arch. Rational Mech. Anal.* **90** (1985) 219–247.
14. E. Cosserat and F. Cosserat, *Théorie des corps déformables*. Librairie Scientifique A. Hermann et Fils [Translation: Theory of deformable bodies, NASA TT F-11 561, 1968] Paris, 1909.

15. R. de Borst, Simulation of strain localization: A reappraisal of the Cosserat continuum, *Engrg. Comp.* **8** (1991) 317–332.
16. R. de Borst, A generalization of J_2 -flow theory for polar continua, *Comp. Meth. Appl. Mech. Eng.* **103** (1992) 347–362.
17. R. de Borst and L. J. Sluys, Localization in a Cosserat continuum under static and loading conditions, *Comp. Meth. Appl. Mech. Engrg.* **90** (1991) 805–827.
18. A. Dietsche, P. Steinmann, and K. Willam, Micropolar elastoplasticity and its role in localization, *Int. J. Plasticity* **9** (1993) 813–831.
19. G. Duvaut, Élasticité linéaire avec couples de contraintes. Théorèmes d'existence, *J. Mec. Paris*, **9** (1970) 325–333.
20. A. C. Eringen, *Microcontinuum Field Theories* (Springer, 1999).
21. A. C. Eringen, Theory of micropolar elasticity, in *Fracture. An Advanced Treatise*, Vol. II, ed. H. Liebowitz (Academic Press, 1968), pp. 621–729.
22. A. C. Eringen and C. B. Kafadar, Polar field theories, in *Continuum Physics*, Vol. IV: *Polar and Nonlocal Field Theories*, ed. A. C. Eringen (Academic Press, 1976), pp. 1–73.
23. A. C. Eringen and E. S. Suhubi, Nonlinear theory of simple micro-elastic solids, *Int. J. Engrg. Sci.* **2** (1964) 189–203.
24. S. Forest, G. Cailletaud and R. Sievert, A Cosserat theory for elastoviscoplastic single crystals at finite deformation, *Arch. Mech.* **49** (1997) 705–736.
25. M. Fuchs and G. Seregin, *Variational Methods for Problems from Plasticity Theory and for Generalized Newtonian Fluids*, Lect. Notes Math., Vol. 1749 (Springer, 2000).
26. V. Gheorghita, On the existence and uniqueness of solutions in linear theory of Cosserat elasticity. I, *Arch. Mech.* **26** (1974) 933–938.
27. V. Gheorghita, On the existence and uniqueness of solutions in linear theory of Cosserat elasticity. II, *Arch. Mech.* **29** (1974) 355–358.
28. V. Girault and P.-A. Raviart, *Finite Element Methods for Navier-Stokes Equations* (Springer, 1986).
29. R. Glowinski, *Numerical Methods for Nonlinear Variational Problems* (Springer, 1984).
30. P. Grammenoudis, Mikropolare Plastizität, Ph.D, Thesis, Department of Mechanics, TU Darmstadt, <http://elib.tu-darmstadt.de/diss/000312>, 2003.
31. P. Grammenoudis and C. Tsakmakis, Hardening rules for finite deformation micropolar plasticity: Restrictions imposed by the second law of thermodynamics and the postulate of Iljuschin, *Cont. Mech. Thermodyn.* **13** (2001) 325–363.
32. A. E. Green and R. S. Rivlin, Multipolar continuum mechanics, *Arch. Rational Mech. Anal.* **17** (1964) 113–147.
33. W. Günther, Zur Statik und Kinematik des Cosseratschen Kontinuums, *Abh. Braunschweigische Wiss. Gesell.* **10** (1958) 195–213.
34. W. Han and B. D. Reddy, *Plasticity: Mathematical Theory and Numerical Analysis* (Springer-Verlag, 1999).
35. I. Hlavacek and M. Hlavacek, On the existence and uniqueness of solutions and some variational principles in linear theories of elasticity with couple-stresses. I: Cosserat continuum. II: Mindlin's elasticity with micro-structure and the first strain gradient, *J. Apl. Mat.* **14** (1969) 387–426.
36. M. M. Iordache and K. Willam, Localized failure analysis in elastoplastic Cosserat continua, *Comp. Meth. Appl. Mech. Engrg.* **151** (1998) 559–586.
37. A. R. Khoei, A. R. Tabarraie and A. A. Gharehbaghi, H -adaptive mesh refinement for shear band localization in elasto-plasticity Cosserat continuum, *Commun. Nonlinear Sci. Numer. Simul.* **10** (2005) 253–286.

38. D. Klatté and B. Kummer, *Nonsmooth Equations in Optimization* (Kluwer, 2002).
39. M. Kojic and K. J. Bathe, *Inelastic Analysis of Solid and Structures* (Springer, 2005).
40. E. Kröner, *Mechanics of Generalized Continua, Proc. of the IUTAM-Symp. on the Generalized Cosserat Continuum and the Continuum Theory of Dislocations with Applications in Freudenstadt*, 1967 (Springer, 1968).
41. R. S. Lakes, On the torsional properties of single osteons, *J. Biomech.* **25** (1995) 1409–1410.
42. S. Lang, C. Wieners and G. Wittum, The application of adaptive parallel multigrid methods to problems in nonlinear solid mechanics, in *Error-Controlled Adaptive Finite Element Methods in Solid Mechanics*, ed. E. Stein (Wiley, 2002), pp. 347–384.
43. H. Lippmann, Eine Cosserat–Theorie des plastischen Fließens, *Acta Mech.* **8** (1969) 255–284.
44. R. D. Mindlin and H. F. Tiersten, Effects of couple stresses in linear elasticity, *Arch. Rational Mech. Anal.* **11** (1962) 415–447.
45. H. B. Mühlhaus, Shear band analysis for granular materials within the framework of Cosserat theory, *Ing. Arch.* **56** (1989) 389–399.
46. H. B. Mühlhaus and E. C. Aifantis, A variational principle for gradient plasticity, *Int. J. Solids Struct.* **28** (1991) 845–857.
47. H. B. Mühlhaus and I. Vardoulakis, The thickness of shear bands in granular material, *Geotech.* **37** (1987) 271–283.
48. P. Neff, The Γ -limit of a finite strain Cosserat model for asymptotically thin domains and a consequence for the Cosserat couple modulus, *Proc. Appl. Math. Mech.* **5** (2005) 629–630.
49. P. Neff, The Cosserat couple modulus for continuous solids is zero viz the linearized Cauchy-stress tensor is symmetric, *Z. Angew. Math. Mech.* **86** (2006) 892–912.
50. P. Neff, Existence of minimizers for a finite-strain micromorphic elastic solid, preprint 2318, *Proc. Roy. Soc. Edinb. A* **136** (2006) 997–1012.
51. P. Neff, A finite-strain elastic-plastic Cosserat theory for polycrystals with grain rotations, *Int. J. Engrg. Sci.* **44** (2006) 574–594.
52. P. Neff, The Γ -limit of a finite strain Cosserat model for asymptotically thin domains versus a formal dimensional reduction, in *Shell-Structures: Theory and Applications*, eds. W. Pietraszkiewicz and C. Szymczak (Taylor and Francis, 2006), pp. 149–152.
53. P. Neff, Finite multiplicative elastic-viscoplastic Cosserat micropolar theory for polycrystals with grain rotations. Modeling and mathematical analysis, preprint 2297, <http://wwwbib.mathematik.tu-darmstadt.de/Math-Net/Preprints/Listen/pp-03.html>, 9/2003.
54. P. Neff and K. Chelminski, A geometrically exact Cosserat shell-model including size effects, avoiding degeneracy in the thin shell limit. Rigorous justification via Γ -convergence for the elastic plate, preprint 2365, <http://wwwbib.mathematik.tu-darmstadt.de/Math-Net/Preprints/Listen/pp04.html>, submitted, 10/2004.
55. P. Neff and K. Chelminski, Infinitesimal elastic-plastic Cosserat micropolar theory. Modelling and global existence in the rate-independent case, *Proc. Roy. Soc. Edinb. A* **135** (2005) 1017–1039.
56. P. Neff and K. Chelminski, Approximation of Prandtl–Reuss plasticity through Cosserat plasticity, preprint 2468, <http://wwwbib.mathematik.tu-darmstadt.de/Math-Net/Preprints/Listen/pp04.html>, submitted to *Quart. Appl. Math.*, 7/2006.
57. P. Neff and K. Chelminski, Well-posedness of dynamic Cosserat plasticity, preprint 2412, <http://wwwbib.mathematik.tu-darmstadt.de/Math-Net/Preprints/Listen/pp-04.html>, to appear in *Appl. Math. Opt.*, 2007.

58. P. Neff, I. Münch and W. Wagner, Constitutive parameters for a nonlinear Cosserat model. A numerical study, Oberwolfach reports 52/2005, European Mathematical Society, 11/2005.
59. N. Oshima, Dynamics of granular media, in *Memoirs of the Unifying Study of the Basic Problems in Engineering Science by Means of Geometry*, Vol. 1, ed. K. Kondo (Gakujutsu Bunken Fukyo-Kai, 1955), pp. 111–120
60. S. I. Repin, Errors of finite element methods for perfect plasticity, *Math. Mod. Meth. Appl. Sci.* **5** (1996) 587–604.
61. M. Ristinmaa and M. Vecchi, Use of couple-stress theory in elasto-plasticity, *Comp. Meth. Appl. Mech. Engrg.* **136** (1996) 205–224.
62. C. Sansour, A theory of the elastic-viscoplastic Cosserat continuum, *Arch. Mech.* **50** (1998) 577–597.
63. C. Sansour, A unified concept of elastic-viscoplastic Cosserat and micromorphic continua, in *Mechanics of Materials with Intrinsic Length Scale: Physics, Experiments, Modeling and Applications*, Journal Physique IV France 8, eds. A. Bertram and F. Sidoroff (EDP Sciences, 1998), pp. 341–348.
64. C. Sansour, Ein einheitliches Konzept verallgemeinerter Kontinua mit Mikrostruktur unter besonderer Berücksichtigung der finiten Viskoplastizität, Habilitation-Thesis, Shaker-Verlag, Aachen, 1999.
65. A. Sawczuk, On the yielding of Cosserat continua, *Arch. Mech. Stosow.* **19** (1967) 471–480.
66. H. Schaefer, Das Cosserat-Kontinuum, *Z. Angew. Math. Mech.* **47** (1967) 485–498.
67. J. C. Simo and T. J. R. Hughes, *Computational Inelasticity* (Springer-Verlag, 1998).
68. P. Steinmann, A micropolar theory of finite deformation and finite rotation multiplicative elastoplasticity, *Int. J. Solids Struct.* **31** (1994) 1063–1084.
69. R. Temam, *Mathematical Problems in Plasticity* (Bordas, 1985).
70. R. Temam, A generalized Norton–Hoff model and the Prandtl–Reuss law of plasticity, *Arch. Rational Mech. Anal.* **95** (1986) 137–183.
71. R. A. Toupin, Elastic materials with couple stresses, *Arch. Rational Mech. Anal.* **11** (1962) 385–413.
72. R. A. Toupin, Theory of elasticity with couple stresses, *Arch. Rational Mech. Anal.* **17** (1964) 85–112.
73. C. Truesdell and W. Noll, The non-linear field theories of mechanics, in *Handbuch der Physik*, Vol. III/3, ed. S. Flügge (Springer, 1965).
74. C. Wieners, Distributed point objects. A new concept for parallel finite elements, in *Domain Decomposition Methods in Science and Engineering, Lecture Notes in Computational Science and Engineering*, Vol. 40, eds. R. Kornhuber *et al.* (Springer, 2004), pp. 175–183.